NASA TECHNICAL NOTE

NASA TN D-3184

NASA TN D-3184

OPTIMIZATION OF DOUBLE-CONIC INTERPLANETARY TRAJECTORIES

by Edward A. Willis, Jr.

Lewis Research Center

Cleveland, Ohio

NATIONAL AERONAUTICS AND SPACE ADMINISTRATION • WASHINGTON, D. C. • JANUARY 1966

NASA TN D-3184

OPTIMIZATION OF DOUBLE-CONIC INTERPLANETARY TRAJECTORIES

By Edward A. Willis, Jr.

Lewis Research Center
Cleveland, Ohio

NATIONAL AERONAUTICS AND SPACE ADMINISTRATION

For sale by the Clearinghouse for Federal Scientific and Technical Information
Springfield, Virginia 22151 – Price $2.00

OPTIMIZATION OF DOUBLE-CONIC INTERPLANETARY TRAJECTORIES

by Edward A. Willis, Jr.

Lewis Research Center

SUMMARY

An efficient class of high-thrust interplanetary trajectories is considered in which each one-way planet-to-planet transfer may consist of two distinct coasting arcs joined by an optimal midcourse impulse. The analysis is based on the successive two-body trajectory model and also assumes low circular parking orbits at each planet, impulsive thrust, and coplanar elliptic planet orbits. The location, direction, and magnitude of the midcourse impulse are optimized directly by a convenient numerical search procedure.

These double-conic trajectories are compared with conventional single-conic trajectories using one-way and stopover round trips to Mars as typical examples with total velocity increment, trip time, and stay time for criteria. It is shown that double-conic trajectories significantly reduce the total velocity increment for one-way transfers which cover heliocentric travel angles greater than 4 radians. Round-trip durations of 300 to 1000 days with stay times of 0 to 140 and 450 days are then studied in 1971 and 1980. A 500-day trip with a 40-day stay time is also investigated over a range of synodic periods from 1971 to 1980. The double-conic trajectories yield attractive reductions in the propulsive velocity increment sum, and/or lower Earth-approach (reentry) velocities, for round-trip times of 360 to 700 days. These advantages are available in all synodic periods, but are most pronounced in the more difficult periods.

INTRODUCTION

Trajectory studies are an essential part of interplanetary mission analysis. Trajectory data are not only used directly in the mission calculations, but criteria such as the total velocity increment $\sum \Delta V$, total trip time T_{tot}, and stay time T_s by themselves provide valuable guidelines for selecting candidate trajectories. For instance, trajectories with minimum $\sum \Delta V$ often yield low if not minimum space vehicle weight.

Previous surveys of high-thrust trajectories, such as references 1 to 3, have assumed that major propulsive maneuvers only occur near a planet terminal. Each one-way heliocentric transfer would then consist of a single coasting arc, and a round trip would consist of two such single-arc transfers. This assumption leads to a convenient numerical computational procedure but not always to

minimum total velocity increments. Rigorous investigations, such as reference 4, have shown that optimal one-way transfers in some cases consist of two coasting arcs joined by a midcourse impulse rather than one single arc. This raises the possibility, not considered in reference 4, that double-arc transfers might also be useful as one or both legs of a round trip. The rigorous variational solutions are valuable as standards of comparison but have not received a wide practical application to high-thrust trajectories because of inherent computational difficulties.

The two objects of this report, therefore, are to develop a more effective technique to find optimal double-arc transfers, and to present examples illustrating the characteristics and utility of this class of trajectories for both one-way transfers and round trips.

The following analysis considers trajectories in which each one-way planet-to-planet transfer may consist of two distinct coasting arcs joined by a midcourse impulse. These are referred to as "double-conic" or "three-impulse" transfers in contrast to the conventional single-conic transfers assumed in references 1 to 3. The two arcs lie in a single plane as opposed to the "broken-plane" transfers discussed in reference 5. The magnitude, direction, and location of the midcourse impulse are optimized with the aid of a direct method (first described in ref. 6) rather than by a variational technique. The present formulation includes single-conic transfers as a special case in which the midcourse impulse vanishes. Also included as a special case is the "perihelion-propulsion" trajectory in which the midcourse impulse occurs at the common perihelion of the two arcs. All previously established optimal results such as the classical Hohmann transfer and the 360° three-impulse transfers discussed in reference 4 are recovered when appropriate boundary conditions are applied. The resulting program is not only computationally efficient, but is also very flexible in that various criteria of merit, boundary conditions, and constraints can be easily accommodated.

A family of potentially desirable Earth-Mars trips is studied as a typical application of this analysis; the velocity increment sum is used as an illustrative criterion of merit. Round trips lasting 300 to 1000 days, with stay times at Mars of 0 to 140 and 450 days, are considered in the oppositions of 1971 and 1980. A 500-day round trip with a 40-day stay is evaluated in all oppositions from 1971 to 1986. The effects of atmospheric braking and trajectory profile are also discussed, and double-conic trajectories are compared with conventional and Venus-swingby trajectories.

SYMBOLS

C coefficient defined in appendix A

D date, Julian day

e eccentricity

M planetary motion, rad/day

N revolution index

T	time, days
ΔT	terminal-to-terminal travel time, days
δT	time error, defined in appendix A
V	velocity, miles/sec
ΔV_n	impulsive velocity increment at terminal n, miles/sec
$\sum_1^n \Delta V_j$	total velocity increment for n impulses, miles/sec
$\langle X \rangle$	denotes time-average of X
α_p	planet perihelion position (see table V)
β	heliocentric travel angle (see fig. 4), rad
η	trajectory true anomaly at planet terminal, measured positive in direction from midcourse maneuver toward planet (see fig. 4, views A and B), rad
θ	orbital true anomaly of planet, measured positive, counterclockwise, rad
κ	travel angle distribution parameter, μ_i/β
μ	partial travel angle (see fig. 4), rad
ν	trajectory true anomaly at midcourse maneuver, measured positive toward planet (see fig. 4, views A and B), rad
ρ	heliocentric radius, astronomical units, or planetocentric radius in planet radii
τ	planet orbital period, days
ψ	trajectory path angle (fig. 4), rad

Subscripts:

e	atmospheric entry
i	inner
inw	inward
k	kick point (i.e., location of midcourse maneuver)

o	outer
out	outward
opp	opposition
p	perihelion
pl	planet
po	parking orbit
r	relative
s	stay
si	sphere of influence
t	trajectory
tot	total
∞	denotes conditions at great distance from center of gravitational force
$\oplus$	Earth
σ	Mars
1	Earth departure
2	outbound kick point
3	Mars arrival
4	Mars departure
5	inbound kick point
6	Earth arrival

ANALYSIS

Several major steps are involved in seeking desirable trajectories:

(1) Criteria of merit must be defined.

(2) An appropriate computational model must be devised.

(3) A suitable optimization technique must be applied to this model to obtain the best possible values of the selected criteria.

These steps will be developed below for one-way and round-trip trajectories

using both single- and double-conic transfers.

Criteria of Merit

Many independent variables must be considered in evaluating final mission criteria such as space vehicle weight or cost. Several useful mission parameters, however, may be studied on the basis of trajectory information alone. These include the following:

(1) The total velocity increment $\sum \Delta V$

(2) The total trip time T_{tot}

(3) For round trips, the stay time T_s at the destination planet

The most important of these is the total velocity increment. The mass ratio required for each propulsive maneuver is directly related to the associated velocity increment, and the sum of these increments is certainly the best single indication of space vehicle weight that can be obtained without making numerous assumptions about the vehicle systems, payloads, and mission objectives. The velocity increment sum is therefore used as the primary criterion of merit for the purpose of developing and illustrating the trajectory optimization procedure. It could easily be replaced by cost, weight, or other criteria in order to study a specific mission or program; this substitution would not involve any essential change in the method of analysis.

The trip and stay times are treated as secondary criteria. A low value of T_{tot} would indicate a minimal exposure to the hazards of space, and for round trips, the stay time limits the time available to accomplish the primary mission objectives.

With these criteria, the optimization procedure to be developed will yield minimum $\sum \Delta V$ one-way transfers which satisfy specified boundary conditions such as travel time and heliocentric travel angle. These optimal one-way transfers may be of interest for probe missions, and are also used to construct minimum $\sum \Delta V$ round trips with prescribed trip time T_{tot} and stay time T_s.

Approximations

This analysis is based on the impulsive two-body trajectory model as described in reference 1; that is, propulsive maneuvers are treated as impulses and the actual n-body problem is replaced by a sequence of two-body coasting arcs. Successive heliocentric arcs are joined by a midcourse impulse; heliocentric and planetocentric arcs are related by matching conditions applied at the "sphere of influence." Inside the sphere of influence, only the planet's gravitational field is considered, and outside, only the Sun's. The spheres of influence are taken to be of negligible size compared to interplanetary distances, but much larger than the parking orbit radii. It is assumed that transfers begin and end in circular planetocentric parking orbits, and that the planets themselves lie in elliptic[1] coplanar heliocentric orbits. As shown in ref-

[1]Circular planet orbits are temporarily used for illustrative purposes in this section, but the data to be presented in the RESULTS AND DISCUSSION are based on elliptic orbits.

erence 5, the $\sum \Delta V$ data for optimal three-dimensional (broken-plane) transfers are well approximated by coplanar elliptic data; this will be discussed later (p. 19).

Under these assumptions, the well-known conic orbit equation (derived in ref. 7, for example) is applicable. The form appropriate to the present analysis is

$$\rho = \frac{\rho_p(1 + e)}{1 + e \cos \theta} \tag{1}$$

Computation of Single-Conic Transfers

Single-conic transfers merit individual attention because they occur frequently as a special case of the more complex double-conic transfers and have several elements in common with them.

The heliocentric portion of a typical one-way single-conic transfer is illustrated in figure 1(a). The space vehicle departs from the inner planet by means of an impulse applied at the circular parking orbit. It pierces the sphere of influence at point 1 and follows the heliocentric arc 1-3, describing a central travel angle β_{out}, and finally encounters the destination planet's sphere of influence (point 3) after the travel time ΔT_{1-3} has elapsed. The transition from heliocentric to planetocentric coordinates is illustrated in figure 1(b). The vehicle follows the planet-approach hyperbola 3-3' from the sphere of influence to the perigee, which is at the desired parking orbit radius. The impulsive thrust ΔV changes the vehicle's velocity from V_p to the local satellite velocity V_{po}.

Heliocentric trajectory. - The planet positions and hence the trajectory terminal conditions β, ρ_o, and ρ_i corresponding to a given travel time and planet encounter date may be computed from elliptic ephemeris data as described in appendix A. These quantities together with the travel time ΔT_{i-o} completely specify the elements of the transfer arc.

The necessary relations are derivable from the basic equation (1). When a trial value η_i is used for the trajectory true anomaly at the inner terminal, the eccentricity is

$$e_t = \frac{\rho_o - \rho_i}{\rho_i \cos \eta_i - \rho_o \cos \eta_o} \tag{2}$$

where the true anomaly at the outer terminal is

$$\eta_o = \eta_i + \beta \tag{3}$$

The trajectory perihelion radius is then

$$\rho_p = \rho_i \frac{1 + e_t \cos \eta_i}{1 + e_t} \tag{4}$$

With equations (2) and (4), the required value of η_i may be determined by iterative solution of the time equation (illustrated here for elliptic arcs):

$$\Delta T_{i-o} = \frac{\tau_\oplus}{2\pi\left(1 - e_t^2\right)}\left[\rho_p(1 + e_t)\right]^{3/2}\left[\frac{2 \tan^{-1}\left(\sqrt{\frac{1 - e_t}{1 + e_t}} \tan \frac{\theta}{2}\right)}{\sqrt{1 - e_t^2}} - \frac{e_t \sin \theta}{1 + e_t \cos \theta}\right]\Bigg|_{\theta=\eta_i}^{\theta=\eta_o=\eta_i+\beta} \tag{5}$$

(The iteration cycle is described in appendix A.) The velocity and path angles for both the trajectory and the planet orbits may then be computed at each encounter from the expressions

$$\tan \psi = \frac{e \sin \theta}{1 + e \cos \theta} \tag{6}$$

$$V = 18.5058\left(\frac{2}{\rho} - \frac{1 - e}{\rho_p}\right)^{1/2} \tag{7}$$

(Equations (5) to (7) are also derived in ref. 7.)

Planetocentric trajectory. - The transition from heliocentric to planetocentric coordinates is illustrated in figure 1(b). Because of the assumption made about the size of the sphere of influence, the planetocentric hyperbolic excess velocity V_∞ may be computed by evaluating the law of cosines at the point of intersection of the trajectory and the planet orbit:

$$V_\infty^2 = V_t^2 + V_{pl}^2 - 2V_t V_{pl} \cos(\psi_t - \psi_{pl}) \tag{8}$$

By the two-body assumption, V_∞ is a constant of the planetocentric motion and may be used in the energy equation to evaluate the impulsive velocity increment

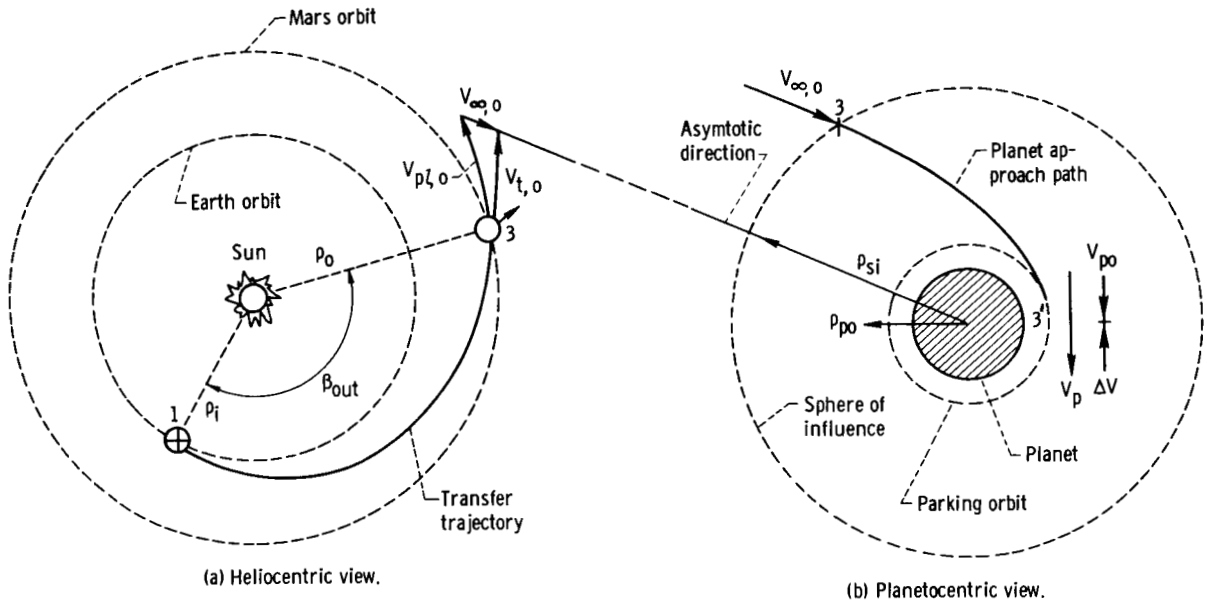

(a) Heliocentric view.

(b) Planetocentric view.

Figure 1. - Typical interplanetary transfer.

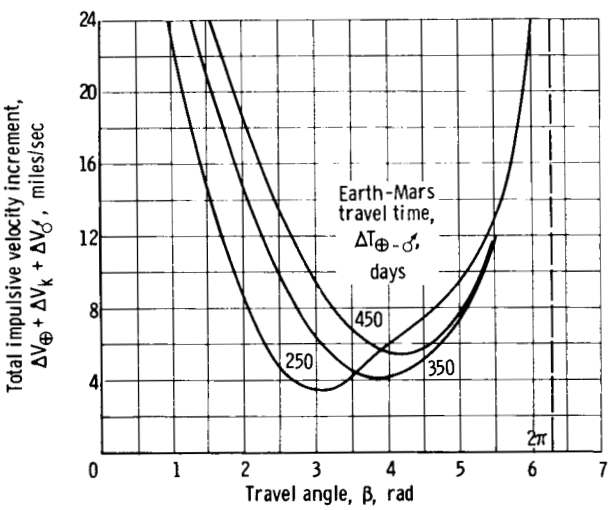

Figure 2. - Characteristics of single-conic Earth-Mars transfers.

required to enter a circular parking orbit whose circular velocity is V_{po}:

$$\Delta V_{pl} = \sqrt{V_\infty^2 + 2V_{po}^2} - V_{po} \qquad (9)$$

(Values of V_{po} corresponding to $\rho_{po} = 1.1$ are listed in table V, appendix A.)

Optimization of Single-Conic Trajectories

One-way transfers. - For a given travel time, the criterion function to be minimized is

$$\sum \Delta V = \Delta V_{pl,i} + \Delta V_{pl,o} \qquad (10)$$

It is important to note, from the foregoing analysis, that a transfer of this kind can be optimized only with respect to two parameters, the travel time ΔT and the travel angle β. (Note that in a given synodic period, and with given ΔT, the choice of the travel angle β is equivalent to choosing the planet encounter date.) The influence of these parameters on $\sum \Delta V$ is illustrated in figure 2 for Earth-Mars transfers in which circular-coplanar planet orbits were assumed for simplicity. The $\sum \Delta V$ is plotted against β for $\Delta T_{\oplus-\sigma'} = 250$, 350, and 450 days. If both β and $\Delta T_{\oplus-\sigma'}$ are left open, optimization yields

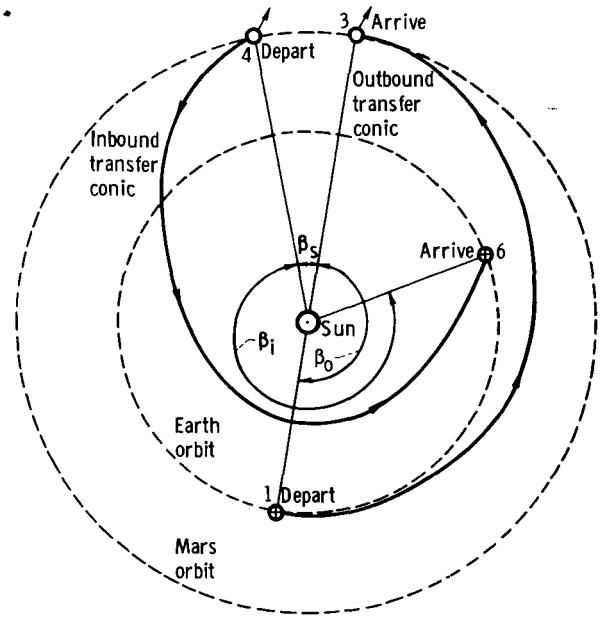

Figure 3. - Typical high-thrust trajectory for Mars round trip. Total trip time, 500 days; stay time, 40 days.

the well-known Hohmann type of transfer. These have a low $\sum \Delta V$ but involve definite values of β and ΔT, which cannot always be incorporated into a desirable round trip. If one parameter (e.g., ΔT) is fixed in advance, then optimization can be only carried out with respect to the remaining one (e.g., β). If both parameters are fixed, then the transfer is completely specified and not subject to any kind of optimization. Note in particular the very high $\sum \Delta V$'s that occur for large values of β.

Round trips. - A round trip consists of two one-way transfers separated by a stopover at the destination planet, as illustrated in figure 3. The complete optimization of a round trip using single-conic transfers would therefore require the determination of the most advantageous travel time and angle for each leg. These must be determined in consistency with the Earth rendezvous condition. That is, since round trips begin and end at Earth, the total angular motion of the space craft during the total trip time T_{tot} must exactly match (within a whole revolution) the Earth's motion during the same time interval:

$$\beta_{out} + \beta_{inw} = \langle M_{\oplus} \rangle T_{tot} - \langle M_{pl} \rangle T_s + 2\pi N \qquad (N = 0, \pm 1, \pm 2, \ldots) \qquad (11)$$

$$\Delta T_{out} + \Delta T_{inw} = T_{tot} - T_s \qquad (12)$$

As the rendezvous condition only needs to be satisfied within whole revolutions, the revolution index N is also subject to choice. A distinct family of round trips corresponds to each choice of N; values of 0 and -1 will be of interest for the Mars trip discussed later (see p. 23.)

"Double-Hohmann" round trips in which the travel times and angles of the outbound and return transfers are optimized independently yield low $\sum \Delta V$ but require specific values of T_{tot} and T_s. When T_{tot} and T_s take on arbitrary values, only two parameters remain free for optimization. Whatever two are used (for instance, the planet encounter date and the outward travel time), the problem ultimately reduces to choosing the optimum distributions of the available travel angle and travel time (cf. eqs. (11) and (12)) between the outward and return legs.

As a highly simplified example, consider a 500-day Earth-Mars round trip with negligible stay time and $N = 0$. (Circular-coplanar planet orbits are still assumed; fig. 2 gives the $\sum \Delta V$ as a function of β and ΔT for both outward and return transfers.) Then, according to equations (11) and (12), the

two travel angles β_{out} and β_{inw} must sum to about 500° or 8.7 radians; the two travel times ΔT_{out} and ΔT_{inw} must add up to 500 days. A natural first trial in seeking the optimum distribution for this trip would be to use the Hohmann outward transfer; this requires $\beta_{out} = 3.14$ radians, $\Delta T_{out} = 250$ days, and $\sum \Delta V_{out} = 3.4$ miles per second as shown on figure 2. The return transfer must then have $\Delta T_{inw} = 250$ days and $\beta_{inw} = 5.56$ radians. With such a long travel angle, a $\sum \Delta V_{inw} = 13.1$ miles per second is required for the return transfer. The grand total for the round trip is then 16.5 miles per second. By similarly evaluating other distributions of travel angle and time, the best round trip is found to consist of symmetric outward and return legs, each having a travel time of 250 days, a travel angle of 4.35 radians, and a $\sum \Delta V$ of 6.8 miles per second. The grand total ΔV for this round trip is then 13.6 miles per second. Neither the outbound nor the return transfer in this example has an individually optimum combination of β and ΔT, yet together they comprise an optimum round trip.

To summarize the foregoing remarks, a single-conic one-way transfer may be optimized only by varying its boundary conditions, that is, β and ΔT. If the transfer is supposed to be part of a round trip, even the possible choices of β and ΔT are restricted by the Earth rendezvous condition.

Computation of Double-Conic Transfers

Double-conic transfers are more responsive to optimization than are the single-conics considered previously. Not only the terminal conditions (β and ΔT) but also the parameters describing the location, magnitude, and direction of the midcourse impulse can be varied. Because of this added flexibility, a double-conic transfer can be optimized to a significant extent even when β and ΔT are fixed.

This section will develop the procedure for computing the elements of a double-conic transfer for arbitrary terminal conditions and an arbitrary midcourse impulse. The following section will then consider optimization of double-conic transfers as applied to both one-way and round trips.

Geometry of double-conic transfers. - Figure 4 illustrates the geometry of a one-way double-conic transfer. As was the case for single-conic transfers, the terminal radii ρ_o and ρ_i and the travel angle β between the terminals are fixed when the planet encounter date D_o and the travel time ΔT are given. The kick impulse ΔV_k occurs at radius ρ_k and divides the transfer into two conic arcs. The arc from the inner terminal covers a central angle μ_i, and it has true anomaly ν_i and path angle $\psi_{k,i}$ at the kick point. Likewise, the outer arc describes a central angle of $\mu_o = \beta - \mu_i$ and has true anomaly ν_o and path angle $\psi_{k,o}$ at the kick point.

Heliocentric trajectory. - The elements of each of the two conic arcs which comprise the heliocentric transfer are uniquely determined by the geometrical

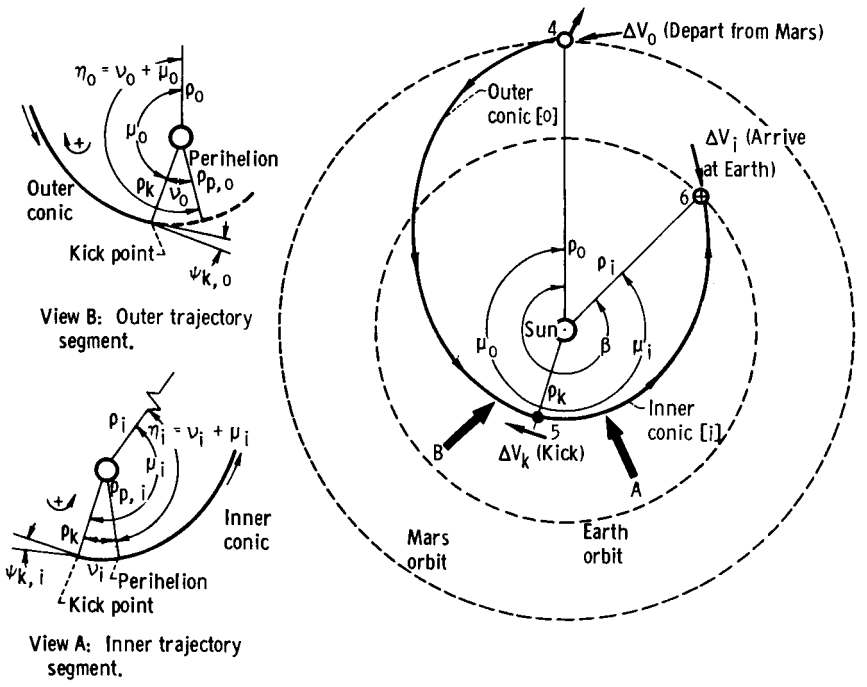

Figure 4. - Geometry of Mars-Earth double-conic trajectory.

quantities ρ_i, μ_i, ρ_o, μ_o, ρ_k, $\psi_{k,i}$, and $\psi_{k,o}$, which were illustrated previously. The necessary relations may be easily derived from the basic equations (1) and (6). The trajectory true anomaly at the inner terminal is

$$\eta_i = \mu_i + \nu_i \tag{13}$$

The eccentricity of the inner arc is then found in terms of ν_i by evaluating equation (1) at the kick point and at the inner terminal and by eliminating ρ_p between the resulting two expressions:

$$e_i = \frac{\rho_i - \rho_k}{\rho_k \cos \nu_i - \rho_i \cos \eta_i} \tag{14}$$

Substituting equation (14) into equation (6), evaluating the result at the kick point, and solving for ν_i yield

$$\nu_i = \tan^{-1}\left[\frac{\tan \psi_{k,i}(1 - \cos \mu_i)}{1 - \frac{\rho_k}{\rho_i} - \sin \mu_i \tan \psi_{k,i}}\right] \text{ rad} \tag{15}$$

when the identity for $\cos(x + y)$ is used. Finally, the perihelion radius of the inner arc is

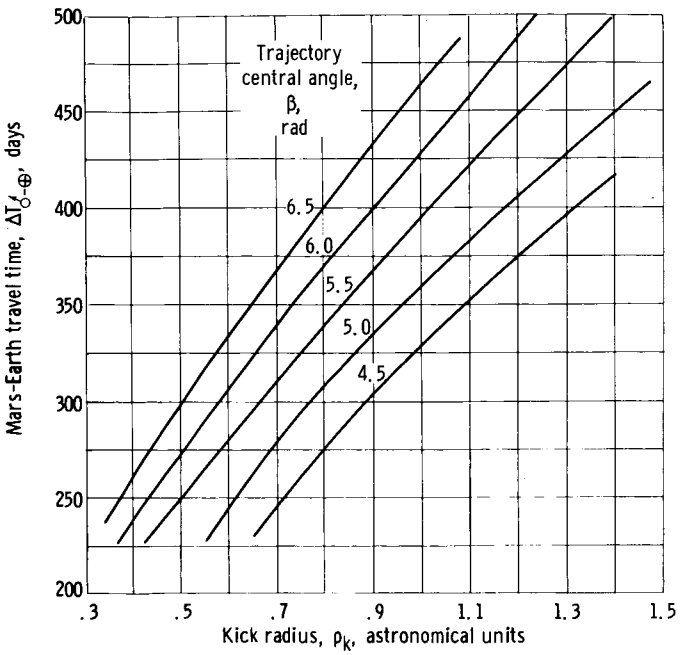

Figure 5. - Mars-Earth transit times for double-conic transfers.

$$\rho_{p,i} = \frac{\rho_k(1 + e_i \cos \nu_i)}{1 + e_i} \qquad (16)$$

The required procedure is then to first compute ν_i, then e_i, and finally $\rho_{p,i}$. The time of transit along the inner arc may then be computed directly from equation (5) evaluated between ν_i and η_i.

These results apply also to the outer subarc (replace subscript i by o) and have the same form whether the original transfer is inward or outward. This follows from the sign convention, illustrated in figure 4, that β and μ are always positive and that true anomalies range from $-\pi$ to π and are measured positive toward the planet associated with each subarc, that is, away from the kick point. (The sign convention for the path angles $\psi_{k,i}$ and $\psi_{k,o}$ is induced by means of eq. (6).) The total travel time for the entire transfer may then be computed by applying equation (5) to both subarcs:

$$\Delta T_{i-o} = \Delta T_i \Big|_{\nu_i}^{\eta_i} + \Delta T_o \Big|_{\nu_o}^{\eta_o} \qquad (17)$$

Equations (13) to (17) specify the transfer in terms of the four independent parameters μ_i, ρ_k, $\psi_{k,i}$, and $\psi_{k,o}$. These, together with the terminal conditions, also implicitly define the midcourse impulse.

One independent parameter must be used to satisfy the travel time constraint. An advantageous choice for this purpose is the kick radius ρ_k. With given values of β, μ_i, ρ_i, $\psi_{k,i}$, ρ_o, and $\psi_{k,o}$, the travel time (eq. (17)) varies monotonically and almost linearly with ρ_k as illustrated in figure 5. Although ρ_k cannot be computed in closed form in terms of ΔT_{i-o}, the required value may be determined from a simple iteration process of the type described in appendix A. For Earth-Mars transfers, a good initial guess for ρ_k may be obtained from figure 5.

The preceding derivation gives the elements e, ρ_p, and ν of a double-conic trajectory which satisfies prescribed terminal conditions and travel time constraint in terms of three independent parameters μ_i, $\psi_{k,i}$, and $\psi_{k,o}$. These parameters implicitly define the midcourse impulse. The magnitude of the midcourse impulse may then be obtained from these elements by evaluating equations

(6) and (7) at the kick point for both the inner and outer arcs and substituting the resulting velocities and path angles into the law of cosines:

$$\Delta V_k = + \left[V_i^2 + V_o^2 - 2V_i V_o \cos (\psi_{k,i} + \psi_{k,o}) \right]^{1/2} \tag{18}$$

Finally, the planetocentric velocity increments are computed from equation (9), just as they were for single-conic transfers.

Optimization of Double-Conic Trajectories

For one-way transfers, the criterion to be minimized is

$$\sum \Delta V = \Delta V_{pl,i} + \Delta V_k + \Delta V_{pl,o} \tag{19}$$

For round trips the object is to minimize the grand total ΔV; that is,

$$\sum \Delta V_{tot} = \sum \Delta V_{out} + \sum \Delta V_{inw} \tag{20}$$

One-way transfer, fixed terminals. - The velocity increment sum for a double-conic transfer can be minimized even when the terminal conditions (defined by ρ_o, ρ_i, β, and ΔT) are prescribed in advance by making use of the extra degrees of freedom associated with the midcourse impulse. The problem is simply to choose the three parameters μ_i, $\psi_{k,i}$, and $\psi_{k,o}$ which control the midcourse impulse so that equation (19) is minimized. An equivalent but more convenient choice of control variables is obtained by the transformation

$$\left.\begin{aligned} \mu_i &= \beta\kappa & 0 \leq \kappa \leq 1 \\ \psi_{k,i} &= \psi_k & -\frac{\pi}{2} \leq \psi_k \leq \frac{\pi}{2} \\ \psi_{k,o} &= \psi_r & -\psi_k, \psi_k - \frac{\pi}{2} \leq \psi_r \leq \psi_k + \frac{\pi}{2} \end{aligned}\right\} \tag{21}$$

Here κ $(= \mu_i/\beta)$ is just the angular location of the kick expressed as a fraction of β, ψ_k is the path angle of the inner arc at the kick point, and ψ_r is the discontinuous change in the path angle in going from the inner arc to the outer. The restrictions on the ranges of the control variables are needed to exclude retrograde arcs.

It should be noted that the control variables are bounded. Thus, an exhaustive investigation of the control space may be made in the search for minimum $\sum \Delta V$. This is an important point since the existence of multiple local minima cannot be ruled out by a priori considerations. A typical example of an exhaustive search is shown in figure 6. Contours of constant $\sum \Delta V$ are plotted on the plane $\psi_r = 0$ of the control space (κ, ψ_k, ψ_r) for a 5.5-radian,

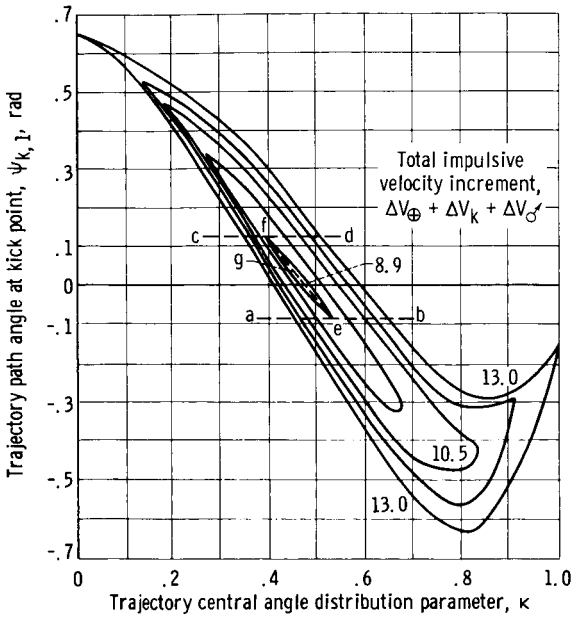

Figure 6. - Velocity-increment contours for 5.5-radian, 250-day, Earth-Mars transfer.

250-day, Mars-Earth transfer. The plane $\psi_r = 0$ is the locus of double-conic transfers using a tangential midcourse impulse. It turns out that these "smooth" transfers are, in fact, optimal for Earth-Mars transfers of practical interest. The heavy curve ($\sum \Delta V$ = 13 miles/sec) forming the left and lower boundary is the trace of the single-conic transfer (i.e., where $\Delta V_k = 0$). This curve is simply a plot of path angle against dimensionless central angle for a heliocentric elliptic arc that traverses 5.5 radians in 250 days. The curve forming the upper and right-hand boundary represents a family of double-conic trajectories that also require 13.0 miles per second. These two curves form a closed contour bounding the region of control space in which double-conic trajectories are more efficient than single conics. The unique minimum of $\sum \Delta V$, 8.9 miles per second, occurs near the center of this contour system where $\psi_k = 0.033$ radian and $\kappa = 0.454$. These values are numerically close to those of the single-conic perihelion for which $\psi_k = 0.0$ and $\kappa = 0.41$, but they decrease the $\sum \Delta V$ by 4.1 miles per second or 30 percent.

Search procedure. - Since the contours of constant $\sum \Delta V$ cannot be represented mathematically in closed form, an efficient numerical search procedure is needed to find the optimal kick impulse controls for the many transfers of interest. One suitable procedure is developed subsequently using the two-dimensional case where $\psi_r = 0$ as an example. (The same basic procedure can also be used for a three-dimensional search where κ, ψ_k, and ψ_r are all varied.)

In the neighborhood of the minimum $\sum \Delta V$ point, the contour system forms a long, narrow, and fairly straight valley. An efficient numerical search procedure for such contours is the method of parallel tangents (PARTAN) as developed in reference 8. A unidimensional search along an arbitrary line, such as a - b in figure 6, yields a relative minimum at point e. A second search along a line c - d (parallel to a - b) yields another relative minimum at f. A third search along the line through e and f yields a candidate minimum at g. If the contours in the neighborhood of the minimum are concentric ellipses, then, as proved in reference 8, point g is the exact center of the contour system, and $\sum \Delta V_g$ is the true minimum. For more general contours, the actual center can be approached within arbitrary tolerances by iterating this procedure starting with a new arbitrary line through g.

Starting the search. - For transfers where $\beta \leq 2\pi$ radians, the single-

conic trajectory may be used to furnish starting conditions that ensure rapid convergence of the PARTAN search cycle. It may be observed from figure 6 that the perihelion, $\psi_{kl} = 0$, is "closer" to the minimum than any other point along the single-conic boundary; this is a natural starting point for the search. The elements of the single-conic transfer may of course be determined as in the preceding section. The coordinates of its perihelion, in the control space, are

$$\left.\begin{aligned} \kappa_p &= -\frac{\eta_i}{\beta} \\ \psi_{k,p} &= 0 \\ \psi_{r,p} &= 0 \end{aligned}\right\} \tag{22}$$

This choice is not possible if the single-conic transfer does not pass through its perihelion. Reasonable initial values then are $\kappa = 0.5$, $\psi_r = 0$, and ψ_k from equation (6). These choices together ensure rapid convergence and guarantee that the search will yield single-conic transfers when those are optimal.

Although not strictly necessary, it is advantageous to take the initial line a - b in the steep descent direction, that is, in the direction of -grad $(\sum \Delta V)$. Then the major part of the saving occurs early in the PARTAN cycle - a time-saving feature for preliminary surveys.

This gradient is perpendicular to the single-conic contour; hence, the slope of a - b for steep descent is

$$\left.\frac{\Delta\psi_k}{\Delta\kappa}\right|_{a\text{-}b} = \left.\frac{-1}{\frac{d\psi}{d\kappa}}\right|_{p,\ \text{single conic}} \tag{23}$$

The necessary derivative may be obtained directly from equation (6) upon noting that

$$\frac{d}{d\kappa} = \beta \frac{d}{d\mu_i} = -\beta \frac{d}{d\nu_i} \tag{24}$$

That is,

$$\frac{d\psi_k}{d\kappa} = -e\beta \cos^2\psi \frac{\cos \nu_i + e}{(1 + e \cos \nu_i)^2} \tag{25}$$

When equation (25) is evaluated at the perihelion, where $\psi_k = \nu_i = 0$, equation (23) becomes

$$\left.\frac{\Delta\psi_k}{\Delta\kappa}\right|_p = \frac{1 + e}{e\beta} \tag{26}$$

This is the steep-descent slope for the initial line a - b, where point a (the single-conic perihelion) is defined by equation (22).

It is considerably more difficult to obtain satisfactory convergence for transfers where $\beta > 2\pi$ radians, since a single-conic transfer cannot be used to obtain a good initial starting point and direction. Such transfers, however, appear to be of little more than academic interest, at least for Mars trips, and will not be further discussed.

Convergence. - At the end of each PARTAN cycle, the candidate minimum at g must be further investigated to be sure that it is actually a minimum and not a saddle or inflection point. A necessary and sufficient condition that $\sum \Delta V$ be minimum at g is that

$$\left.\begin{aligned} &\frac{\partial f}{\partial \kappa} = \frac{\partial f}{\partial \psi_k} = 0 \\ &\frac{\partial^2 f}{\partial \kappa^2} > 0 \\ \text{and} \quad &\frac{\partial^2 f}{\partial \kappa^2}\frac{\partial^2 f}{\partial \psi_k^2} - \left(\frac{\partial^2 f}{\partial \kappa\, \partial \psi_k}\right)^2 > 0 \end{aligned}\right\} \tag{27}$$

where

$$\sum \Delta V = f(\kappa, \psi_k) = f_g + \left.\frac{\partial f}{\partial \kappa}\right|_g \Delta\kappa + \left.\frac{\partial f}{\partial \psi_k}\right|_g \Delta\psi_k + \frac{1}{2}\left(\left.\frac{\partial^2 f}{\partial \kappa^2}\right|_g \Delta\kappa^2 + 2\left.\frac{\partial^2 f}{\partial \psi_k\, \partial \kappa}\right|_g \Delta\psi_k \Delta\kappa + \left.\frac{\partial^2 f}{\partial \psi_k^2}\right|_g \Delta\psi_k^2\right) + \cdots \tag{28}$$

The necessary partials may be numerically approximated, by the usual algebraic means, after computing five test points in a small neighborhood of g. If the conditions of equation (27) are satisfied within acceptable tolerances, the search is terminated at g; if not, it is iterated until they are by using a new initial line through g. It is convenient to place the new initial lines in the steep descent direction also, since the slope of the gradient is just

$$\left.\frac{\Delta\psi_k}{\Delta\kappa}\right|_{\substack{\text{initial,}\\ \text{new line}}} \approx \frac{\dfrac{\partial f}{\partial \kappa}}{\dfrac{\partial f}{\partial \psi_k}} \tag{29}$$

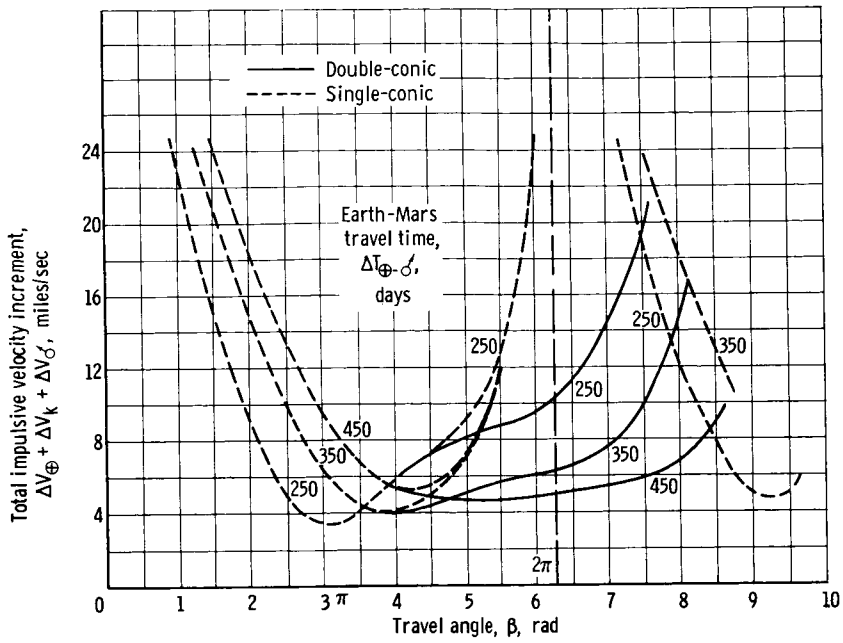

Figure 7. - Comparison of single- and double-conic Earth-Mars transfers.

and the required partial derivatives are already available in equation (27).

One-way transfers; variable terminals. - The preceding discussion considered the optimization of one-way transfers with fixed terminals defined by β and ΔT. Further reductions in $\sum \Delta V$ may be expected for double-conic transfers in those cases where the terminal conditions (β and ΔT) may be optimized in addition to the midcourse impulse. As was the case for single-conic transfers, an optimum value of β occurs for each choice of ΔT; and if both β and ΔT are left open, an overall minimum $\sum \Delta V$ exists for one specific combination of these parameters. These facts, plus a general comparison of single- and double-conic transfers to Mars, are illustrated in figure 7. Again, circular coplanar planet orbits were assumed for simplicity with $\rho_{\sigma'} = 1.53$ astronomical units; the ΔV sum is plotted against the travel angle β for travel times of 250, 350, and 450 days. The single-conic transfers indicated by dashed lines are the same ones that were shown before in figure 2.

Double-conic transfers, denoted by the solid curves, show a sizable advantage compared to single conics in the long travel-angle region. The reduction in $\sum \Delta V$ becomes noticeable at $\beta \approx 4$ radians, reaches a maximum for $\beta = 2\pi$ radians, and extends out to $\beta = 7$ or 8 radians. If β is outside these limits, the results of the double-conic optimization procedure reduce to single-conic transfers. For instance, the optimum ΔV_k approaches 0 continuously as β approaches about 4 radians from above.

For long travel times (over 350 days) a new minimum value of $\sum \Delta V$, lower than the single-conic minimum, occurs in the long-angle region. The corresponding optimum value of β is also greater than it was for the single-conic transfer. For shorter travel times (under 350 days), the optimum trajectories reduce to single-conics before the best value of β is reached. In particular, when both β and ΔT are left open, the classical single-conic Hohmann transfer is

recovered.

In summary, the two characteristic properties of double-conic transfers are as follows: (1) For all travel times, the optimal double-conic transfers require significantly lower $\sum \Delta V$ than the corresponding single-conic transfer, if the travel angle β is required to be larger than about 4 radians, and (2) for shorter angles, the kick impulse ΔV_k vanishes, and the optimal double-conic transfers reduce to single conics.

From these observations, it may be anticipated that double-conic transfers will be of the greatest utility where external constraints, such as the Earth rendezvous condition for round trips, preclude the selection of both optimum β and ΔT.

Round trips. - A round trip in which a double conic is used for either the inward or outward transfer, or both, is referred to herein as a double-conic round trip. Two main steps are required to optimize a round trip in which double-conic transfers may be used: (1) For each trial distribution of β and ΔT, both one-way legs must be optimized as described previously, and (2) the optimal distribution of β and ΔT must then be found in consistency with the Earth rendezvous condition. As was the case when single-conic transfers were used, the rendezvous condition (eqs. (11) and (12)) implies that a round trip with arbitrary values of T_{tot} and T_s, and $N = 0$, must include at least one long-angle transfer. It is of interest to reconsider the 500-day, zero-stay-time Mars round trip that was used as an example previously. Again, the two travel angles must total 8.7 radians; beginning with the Hohmann outward transfer ($\beta = 3.14$ rad, $\Delta T_{out} = 250$ days, and $\sum \Delta V_{out} = 3.4$ miles/sec), the return transfer must have $\Delta T_{inw} = 250$ days and $\beta_{inw} = 5.56$ radians. From figure 7, the $\sum \Delta V_{inw}$ is then 8.9 miles per second for a grand total of 12.3 miles per second. This is already a substantial reduction (1.3 miles/sec) over the minimal single-conic round trip for which $\sum \Delta V_{tot}$ was 13.6 miles per second. It is of interest to note that if double-conic transfers had been applied with the same time and angle distribution that were found optimal for the single-conic trip ($\beta = 4.35$ rad and $\Delta T = 250$ days for each leg), only a small improvement would have been found. This simple and incomplete example is sufficient to illustrate (1) that reoptimization of the travel times and angles is required to develop the full potential advantage of double-conic trajectories, and (2) that the resulting optimal distributions are considerably different than those found for single-conic trajectories.

Computational Technique

The procedures and equations indicated above were programmed for numerical solution on a high-speed digital computer. Planet orbit-element and physical data were taken from reference 3. The resulting program may be used for the computation and optimization of single- and/or double-conic one way and round trips between any combination of planets. Optimization criteria other than $\sum \Delta V$, such as space vehicle weight or cost, could be accommodated without requiring a basic reformulation of the method.

RESULTS AND DISCUSSION

Families of one-way transfers and round trips to Mars were studied as a typical application of the present analysis. The illustrative examples discussed in the preceding section assumed circular planet orbits, but planet-orbit eccentricities are accounted for in the data presented here. The results illustrate the main features of double-conic trajectories and may be directly compared with previous results (refs. 1 to 3), which were based on single-conic transfers.

One-Way Transfers

One-way transfers are of direct interest for probe missions and are also the basis for constructing round trips.

A spectrum of potentially desirable outward and return transfers in 1979 to 1980 is presented in tables I and II. The 1980 synodic period was chosen for discussion because it is one of the more "difficult" periods and is among the earliest in which a manned round-trip mission to Mars might be contemplated.

The data shown were computed on the basis of minimum $\sum \Delta V$ and will be used later to construct round trips with minimum $\sum \Delta V$. These data can also be used for preliminary gross weight and other mission calculations.

Table I lists the parameters of interst for single-conic outward transfers, that is, $\sum \Delta V$, the individual velocity increments, the travel angle, and the minimum solar approach radius, for travel times ranging from 140 to 280 days, and for Mars encounter dates ranging from Julian day 2444380 to 2444460. The corresponding parameters are listed in table II for double-conic inward transfers with travel times of 220 to 270 days and Mars encounter dates from 2444420 to 2444500. The data in table I can also, with little error, be associated with certain inward transfers, and the table II data associated with a group of outward transfers. The reasons why this is true and the procedure for doing so are discussed in appendix B. Direct use of the tables I and II data will result in a family of "short-long" round trips in which the long-angle double-conic leg occurs last. The "long-short" round trips associated with the alternate interpretation then use the long-angle double-conic transfers as the outbound leg. These two types of round trips are compared later (see p. 29).

Effect of planet-orbit inclination. - The outward transfers listed in table I involve short travel angles, for which single-conic transfers are optimal. These data may therefore be compared directly with the results of references 2 and 5, in which inclination effects are considered. This comparison is presented in figure 8, in which $\sum \Delta V$ is plotted against Mars encounter date (and travel angle) for an Earth-to-Mars travel time of 200 days. The coplanar-elliptic results of the present analysis are shown by the solid curve. The dashed curve indicates the results of reference 2, in which a three-dimensional trajectory is assumed to lie in a single transfer plane. These correspond very closely to the present results except near a travel angle of π radians. In this region, the single transfer plane must be inclined nearly

TABLE I. - CHARACTERISTICS OF OPTIMAL EARTH-TO-MARS TRAJECTORIES FOR 1980

Total velocity increment, $\sum_1^3 \Delta V_i$, miles/sec	Earth departure		Kick, ΔV_2, miles/sec	Mars arrival		Minimum radius, ρ_{min}, astronomical units	Central angle, β, rad	Transit time, $T_{\oplus-\sigma}$, days	Julian date at Mars arrival
	ΔV_1, miles/sec	$V_{\infty 1}$, miles/sec		ΔV_3, miles/sec	$V_{\infty 3}$, miles/sec				
6.861	3.190	4.256	--	3.667	4.927	0.983	1.663	140	2444380
6.427	2.813	3.510	--	3.611	4.802	.984	1.841	150	
6.136	2.578	2.977	--	3.555	4.797	.985	2.018	160	
5.945	2.454	2.660	--	3.488	4.719	.986	2.195	170	
5.822	2.412	2.545	--	3.408	4.625	.988	2.372	180	
5.738	2.428	2.589	--	3.308	4.055	.986	2.548	190	
5.675	2.484	2.738	--	3.189	4.363	.980	2.722	200	
5.623	2.506	2.948	--	3.054	4.201	.972	2.897	210	
5.578	2.669	3.191	--	2.907	4.071	.962	3.070	220	
6.901	3.686	5.116	--	3.212	4.392	0.983	1.565	140	2444390
6.313	3.154	4.190	--	3.156	4.325	.983	1.742	150	
5.906	2.783	3.445	--	3.120	4.281	.984	1.920	160	
5.633	2.543	2.890	--	3.087	4.241	.985	2.098	170	
5.434	2.409	2.536	--	3.042	4.186	.986	2.275	180	
5.342	2.354	2.378	--	2.985	4.117	.988	2.451	190	
5.271	2.358	2.389	--	2.911	4.025	.987	2.627	200	
5.223	2.403	2.520	--	2.816	3.908	.983	2.802	210	
5.188	2.478	2.724	--	2.707	3.771	.976	2.976	220	
6.426	3.644	5.048	--	2.779	3.862	0.983	1.645	150	2444400
5.869	3.132	4.149	--	2.734	3.805	.983	1.823	160	
5.480	2.766	3.410	--	2.711	3.777	.984	2.001	170	
5.218	2.524	2.841	--	2.692	3.753	.985	2.178	180	
5.048	2.380	2.455	--	2.665	3.718	.986	2.356	190	
4.940	2.314	2.258	--	2.623	3.665	.988	2.532	200	
4.878	2.307	2.235	--	2.508	3.594	.989	2.708	210	
4.840	2.343	2.345	--	2.495	3.500	.985	2.883	220	
4.822	2.411	2.541	--	2.407	3.386	.978	3.057	230	
6.041	3.607	4.987	--	2.431	3.417	0.983	1.727	160	2444410
5.508	3.114	4.115	--	2.391	3.364	.983	1.905	170	
5.133	2.756	3.387	--	2.374	3.342	.984	2.083	180	
4.872	2.512	2.811	--	2.364	3.328	.985	2.261	190	
4.712	2.362	2.403	--	2.347	3.306	.986	2.438	200	
4.608	2.288	2.174	--	2.318	3.267	.988	2.614	210	
4.551	2.271	2.120	--	2.278	3.213	.989	2.790	220	
4.521	2.298	2.207	--	2.221	3.136	.987	2.965	230	
4.512	2.359	2.393	--	2.151	3.040	.981	3.139	240	
5.734	3.575	4.934	--	2.156	3.048	0.983	1.810	170	2444420
5.217	3.100	4.089	--	2.114	2.989	.983	1.988	180	
4.850	2.760	3.374	--	2.098	2.966	.984	2.106	190	
4.599	2.506	2.797	--	2.091	2.956	.985	2.343	200	
4.435	2.352	2.373	--	2.080	2.941	.986	2.521	210	
4.333	2.270	2.117	--	2.060	2.914	.988	2.697	220	
4.279	2.245	2.033	--	2.031	2.872	.990	2.873	230	
4.254	2.265	2.099	--	1.987	2.809	.988	3.048	240	
4.254	2.319	2.273	--	1.932	2.730	.983	3.222	250	
5.490	3.544	4.881	--	1.944	2.748	0.983	1.894	180	2444430
4.985	3.086	4.061	--	1.897	2.678	.983	2.072	190	
4.623	2.744	3.361	--	1.877	2.649	.984	2.250	200	
4.374	2.502	2.787	--	1.869	2.636	.985	2.427	210	
4.209	2.345	2.353	--	1.861	2.625	.986	2.605	220	
4.108	2.258	2.078	--	1.847	2.604	.988	2.781	230	
4.055	2.227	1.970	--	1.825	2.572	.990	2.957	240	
4.034	2.240	2.016	--	1.792	2.521	.989	3.132	250	
4.041	2.289	2.179	--	1.749	2.456	.984	3.306	260	
5.298	3.508	4.820	--	1.788	2.515	0.983	1.979	190	2444440
4.801	3.068	4.030	--	1.731	2.427	.983	2.157	200	
4.443	2.736	3 344	--	1.704	2.385	.984	2.335	210	
4.193	2.499	2.777	--	1.692	2.366	.985	2.513	220	
4.028	2.341	2.339	--	1.684	2.354	.986	2.690	230	
3.926	2.250	2.050	--	1.673	2.336	.988	2.866	240	
3.874	2.214	1.923	--	1.657	2.311	.990	3.042	250	
3.857	2.222	1.953	--	1.632	2.271	.989	3.217	260	
3.872	2.267	2.108	--	1.600	2.218	.985	3.391	270	
5.799	4.003	5.621	--	1.796	2.527	0.984	1.888	190	2444450
5.148	3.469	4.754	--	1.677	2.343	.983	2.066	200	
4.659	3.048	3.988	--	1.610	2.233	.983	2.244	210	
4.303	2.726	3.321	--	1.575	2.175	.984	2.422	220	
4.053	2.493	2.763	--	1.557	2.146	.985	2.599	230	
3.885	2.336	2.325	--	1.547	2.128	.986	2.776	240	
3.782	2.244	2.029	--	1.536	2.111	.988	2.953	250	
3.730	2.204	1.889	--	1.524	2.090	.990	3.128	260	
3.717	2.209	1.907	--	1.505	2.058	.990	3.303	270	
5.672	3.935	5.514	--	1.735	2 434	0.984	1.976	200	2444460
5.034	3.426	4.679	--	1.606	2.227	.983	2.154	210	
4.552	3.023	3.939	--	1.527	2.095	.983	2.332	220	
4.197	2.713	3.292	--	1.482	2.018	.984	2.509	230	
3.946	2.486	2.744	--	1.458	1.978	.985	2.687	240	
3.777	2.331	2.310	--	1.444	1.949	.986	2.864	250	
3.673	2 238	2.010	--	1.433	1.930	.988	3.041	260	
3.621	2.198	1.864	--	1.423	1.911	.990	3.216	270	
3.612	2.201	1.875	--	1.411	1.887	.990	3.391	280	

TABLE II. - CHARACTERISTICS OF OPTIMAL MARS-TO-EARTH TRAJECTORIES FOR 1980

Julian date at Mars departure	Transit time, $T_{\sigma-\oplus}$, days	Total velocity increment, $\sum_4^6 \Delta V_i$, miles/sec	Mars departure		Kick, ΔV_5, miles/sec	Earth arrival		Minimum radius, ρ_{min}, astronomical units	Central angle, β, rad
			ΔV_4, miles/sec	$V_{\infty 4}$, miles/sec		ΔV_6, miles/sec	$V_{\infty 6}$, miles/sec		
2444420	220	9.771	3.611	4.862	1.566	4.595	6.498	0.548	4.912
	230	9.202	3.414	4.631	1.767	4.022	5.650	.546	5.089
	240	8.745	3.189	4.364	1.802	3.753	5.225	.540	5.265
	250	8.369	3.074	4.225	1.924	3.371	4.583	.539	5.440
	260	8.081	2.968	4.095	2.001	3.113	4.113	.539	5.615
	270	7.860	2.915	4.030	2.118	2.826	3.538	.543	5.788
	280	7.716	2.830	3.925	2.175	2.712	3.290	.542	5.961
	290	7.620	2.724	3.793	2.298	2.598	3.025	.552	6.132
	300	7.597	2.696	3.758	2.358	2.543	2.890	.550	6.303
2444430	210	10.424	4.004	5.315	1.526	4.894	6.918	0.542	4.828
	220	9.749	3.650	4.907	1.617	4.482	6.336	.531	5.005
	230	9.190	3.490	4.721	1.829	3.870	5.413	.531	5.181
	240	8.744	3.263	4.453	1.839	3.642	5.044	.527	5.357
	250	8.387	3.144	4.310	1.936	3.307	4.469	.526	5.531
	260	8.112	3.077	4.228	2.056	2.979	3.853	.529	5.704
	270	7.922	2.982	4.113	2.115	2.825	3.537	.529	5.877
	280	7.880	2.731	3.802	2.383	2.766	3.410	.553	6.048
	290	7.738	2.831	3.926	2.304	2.603	3.038	.536	6.219
2444440	210	10.387	3.972	5.278	1.509	4.905	6.933	0.521	4.920
	220	9.735	3.650	4.908	1.572	4.514	6.381	.515	5.096
	230	9.182	3.570	4.814	1.870	3.742	5.208	.518	5.271
	240	8.746	3.395	4.609	1.938	3.413	4.656	.516	5.446
	250	8.416	3.220	4.401	1.944	3.252	4.370	.512	5.619
	260	8.164	3.149	4.316	2.053	2.961	3.817	.515	5.792
	270	7.999	3.054	4.201	2.122	2.823	3.532	.516	5.963
	280	7.901	2.992	4.126	2.195	2.713	3.293	.516	6.134
	290	7.892	2.916	4.032	2.352	2.625	3.089	.526	6.303
2444450	200	11.136	4.301	5.650	1.309	5.526	7.770	0.508	4.833
	210	10.353	4.020	5.333	1.561	4.772	6.748	.505	5.010
	220	9.708	3.732	5.003	1.643	4.333	6.118	.500	5.185
	230	9.182	3.555	4.797	1.768	3.858	5.394	.499	5.359
	240	8.766	3.425	4.645	1.877	3.464	4.744	.499	5.533
	250	8.449	3.337	4.541	1.991	3.120	4.127	.502	5.705
	260	8.231	3.226	4.409	2.048	2.956	3.808	.502	5.877
	270	8.108	3.177	4.349	2.095	2.836	3.560	.500	6.047
	280	8.033	3.058	4.205	2.293	2.683	3.223	.515	6.217
2444460	200	11.093	4.391	5.752	1.434	5.269	7.428	0.494	4.922
	210	10.326	4.030	5.344	1.527	4.769	6.744	.488	5.097
	220	9.689	3.821	5.105	1.692	4.177	5.885	.486	5.271
	230	9.186	3.638	4.893	1.782	3.766	5.247	.486	5.445
	240	8.792	3.514	4.749	1.885	3.393	4.621	.487	5.617
	250	8.505	3.416	4.633	1.979	3.110	4.108	.489	5.789
	260	8.316	3.309	4.507	2.042	2.965	3.825	.487	5.959
	270	8.204	3.245	4.431	2.148	2.811	3.507	.491	6.129
	280	8.197	3.103	4.260	2.405	2.688	3.236	.510	6.298
2444470	200	11.057	4.505	5.879	1.543	5.009	7.077	0.482	5.008
	210	10.298	4.108	5.433	1.509	4.621	6.535	.474	5.182
	220	9.680	3.964	5.269	1.783	3.933	5.511	.477	5.356
	230	9.199	3.733	5.003	1.795	3.672	5.093	.473	5.528
	240	8.833	3.608	4.859	1.889	3.336	4.522	.475	5.699
	250	8.576	3.500	4.732	1.969	3.107	4.102	.475	5.870
	260	8.429	3.436	4.658	2.026	2.967	3.829	.470	6.040
	270	8.360	3.311	4.510	2.279	2.772	3.423	.493	6.208
	280	8.388	3.121	4.282	2.565	2.702	3.267	.506	6.377
2444480	200	11.016	4.495	5.868	1.494	5.027	7.100	0.464	5.091
	210	10.275	4.213	5.551	1.624	4.439	6.272	.462	5.265
	220	9.684	4.055	5.373	1.788	3.841	5.366	.464	5.437
	230	9.227	3.874	5.166	1.848	3.505	4.815	.464	5.609
	240	8.890	3.712	4.980	1.893	3.285	4.430	.463	5.779
	250	8.669	3.592	4.840	1.957	3.120	4.127	.461	5.949
	260	8.538	3.493	4.724	2.157	2.889	3.669	.476	6.118
	270	8.546	3.331	4.534	2.440	2.774	3.428	.491	6.286
	280	8.588	3.080	4.233	2.787	2.721	3.309	.501	6.453
2444490	200	10.988	4.563	5.943	1.508	4.918	6.951	0.450	5.172
	210	10.271	4.268	5.614	1.590	4.413	6.235	.448	5.345
	220	9.703	4.091	5.413	1.713	3.897	5.454	.447	5.516
	230	9.271	3.963	5.268	1.831	3.477	4.767	.451	5.687
	240	8.967	3.805	5.071	1.877	3.284	4.428	.450	5.856
	250	8.786	3.706	4.972	1.942	3.138	4.161	.446	6.025
	260	8.761	3.567	4.811	2.349	2.845	3.580	.480	6.193
	270	8.773	3.326	4.527	2.665	2.782	3.445	.489	6.361
	280	8.807	2.937	4.057	3.092	2.779	3.437	.493	6.528
2444500	190	11.838	4.981	6.405	1.374	5.483	7.713	0.439	5.078
	200	10.971	4.641	6.031	1.513	4.817	6.810	.437	5.251
	210	10.282	4.337	5.691	1.558	4.387	6.197	.436	5.422
	220	9.733	4.189	5.524	1.703	3.841	5.366	.436	5.593
	230	9.333	4.056	5.362	1.796	3.491	4.791	.438	5.762
	240	9.065	3.905	5.201	1.864	3.296	4.450	.436	5.931
	250	8.925	3.804	5.085	2.119	3.003	3.901	.455	6.099
	260	8.958	3.591	4.839	2.501	2.867	3.624	.474	6.268
	270	8.961	3.263	4.452	2.873	2.823	3.533	.481	6.434

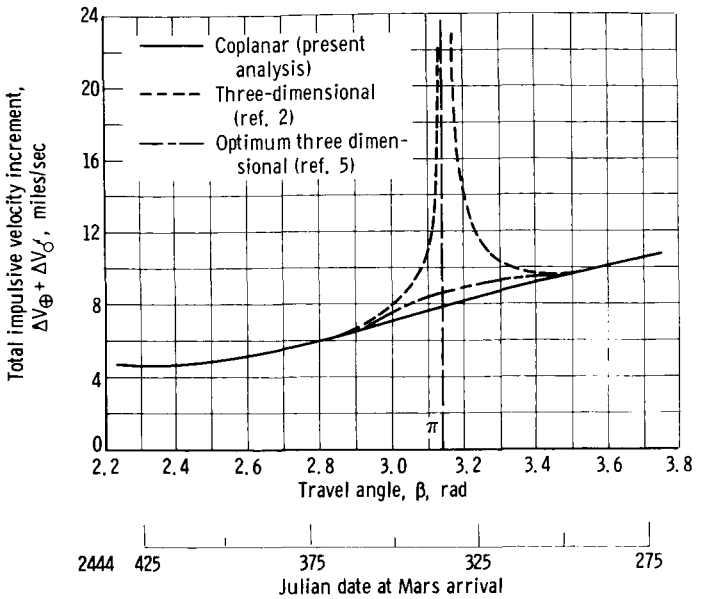

Figure 8. - Comparison of coplanar and three-dimensional results for Earth-Mars trips. Earth-Mars travel time, 200 days.

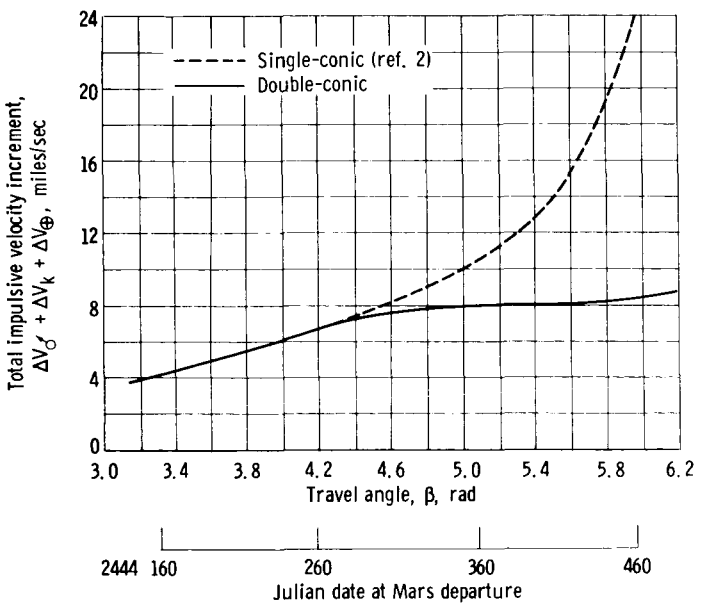

Figure 9. - Characteristics of double-conic Mars-Earth transfers in 1980. Mars-Earth travel time, 260 days.

normal to the ecliptic in order to include the Earth, Sun, and Mars; the associated $\sum \Delta V$ is unrealistically high. The optimal three-dimensional trajectory for this case is a broken-plane transfer as described in reference 5 and indicated by the dotted curve on figure 8. It may be seen from this comparison that the present coplanar results are actually a better approximation to optimal three-dimensional transfers than are the single-plane transfers of reference 2.

Characteristics of double-conic transfers. - The inward transfers shown in table II involve long travel angles; they are double-conic trajectories in which the midcourse impulse was chosen to minimize $\sum_4^6 \Delta V$. These transfers result in a sizable reduction in $\sum_4^6 \Delta V$ as compared to single-conic trajectories. This is illustrated in figure 9, where $\sum \Delta V$ is plotted against Mars departure date (and travel angle) for 260-day single-conic (dashed line) and double-conic inward transfers (solid curve). As was the case with the circular-coplanar data used in illustrating the search procedure, the double-conic transfers become advantageous for travel angles greater than about 4 radians; the corresponding departure date is 2444220. The advantage increases rapidly for larger travel angles (later departure dates). For instance, a double-conic 260-day trip departing on 2444460 (β = 5.96 rad) requires a $\sum \Delta V$ of only 8.3 miles per second, while the equivalent single-conic requires nearly 20 miles per second.

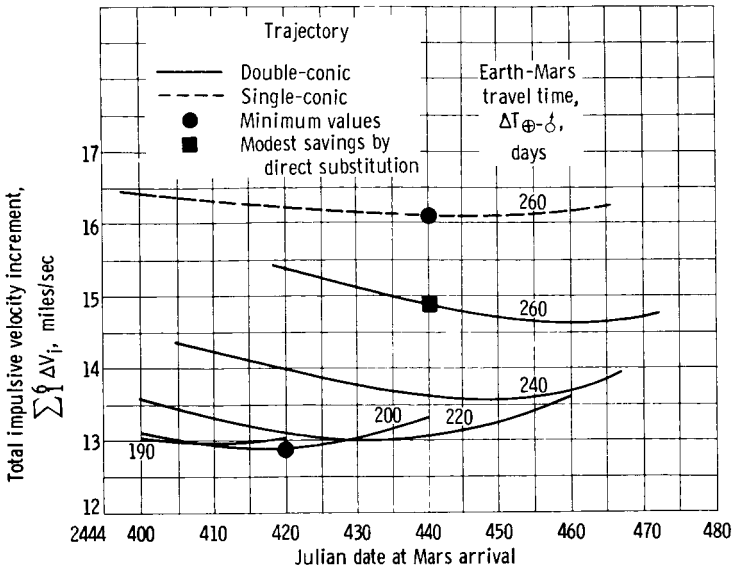

Figure 10. - Mars round-trip optimization. Total trip time, 500 days; stay time, 40 days; low circular parking orbits.

Round Trips

The optimal one-way transfer data presented in tables I and II may be used for the construction of round trips. All that remains is to select the best distribution of travel time and angle between the outward and return legs, for each desired trip time and stay time at Mars. The selection of the travel time and angle distribution is equivalent to the selection of the date of Mars encounter and the outward travel time. Consider, for instance, a 500-day round trip with a 40-day stay at Mars. Choosing an arrival date $D_{\sigma'} = 2444420$ and $\Delta T_{\oplus-\sigma'} = 200$ days, it may be seen in table I that $\sum_1^3 \Delta V = 4.599$ miles per second for the outward transfer (assuming propulsive braking at Mars). The return transfer thus departs Mars on 2444460 and has a travel time of 260 days; from table II, the corresponding $\sum_4^6 \Delta V = 8.316$ miles per second, with propulsive braking at Earth. Hence, for this particular round trip, the $\sum_1^6 \Delta V = 12.915$ miles per second. By repeating this procedure, the most favorable arrival date and travel time may be found as illustrated in figure 10. The $\sum \Delta V$ for all propulsive single-conic (dashed curves) and double-conic (solid curves) round-trip durations of 500 days with 40-day stay is plotted against Mars arrival date. In each case, the minimum value is denoted by the circle symbols. The full ΔV savings of 3.2 miles per second is developed at an arrival data and travel times considerably different from those which were best for single-conic transfers (a modest saving, the square symbol, is still available when double-conic transfers are substituted directly into a minimum $\sum \Delta V$ single-conic round trip without reoptimizing the dates and travel times). The overall effect of the reoptimization is to allocate a larger travel time and angle to the long-angle return transfer, thus taking full advantage of the favorable low $\sum \Delta V$ at long travel angle characteristic of double-conic transfers.

The minimum $\sum \Delta V$ single- and double-conic trajectories in figure 10

TABLE III. - COMPARISON OF OPTIMAL SINGLE- AND DOUBLE-CONIC ROUND TRIPS IN 1980

[Total trip time, 500 days; stay time, 40 days.]

Type of trajectory	Minimum total velocity increment, $\sum_1^6 \Delta V$, miles/sec	Outward transfer					Return transfer				
		Earth-Mars travel time, $\Delta T_{\oplus-\sigma'}$, days	Earth-Mars travel angle, $\beta_{\oplus-\sigma'}$, rad	Impulsive velocity increment, miles/sec			Mars-Earth travel time, $\Delta T_{\sigma'-\oplus}$, days	Mars-Earth travel angle, $\beta_{\sigma'-\oplus}$, rad	Impulsive velocity increment, miles/sec		
				At Earth, ΔV_1	At kick point, ΔV_2	At Mars, ΔV_3			At Mars, ΔV_4	At kick point, ΔV_5	At Earth, ΔV_6
Single-conic	16.3	260	3.13	2.20	0	1.50	200	5.17	4.25	0	8.35
Double-conic	12.9	200	2.34	2.40	0	2.30	260	5.96	3.25	2.0	2.95

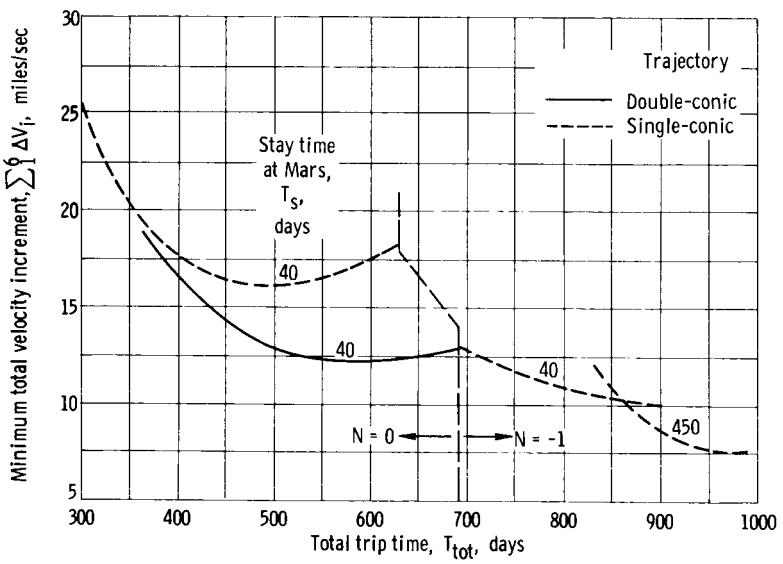

Figure 11. - Comparison of single- and double-conic round trips to Mars. All propulsive braking (1980).

are further compared in table III. It is of interest to note that, with single-conic transfers, the individual velocity increments vary from 1.5 to 8.35 miles per second, while with double-conics the variation is only between 2 and 3.25 miles per second. It may be inferred from the ΔV_6 data (Earth return) that an extremely high (about 70 000 ft/sec) Earth aerobraking capability would be required to make the single-conic trajectory competitive with the double-conic.

Effect of total trip time. - In the preceding example, the use of double-conic transfers was seen to produce a large reduction in $\sum \Delta V$ for a 500-day trip time. It is also of interest to consider how the available savings varies as a function of the total trip time. In figure 11, the $\sum \Delta V$ is plotted against total trip time for all-propulsive, single- and double-conic trajecto-

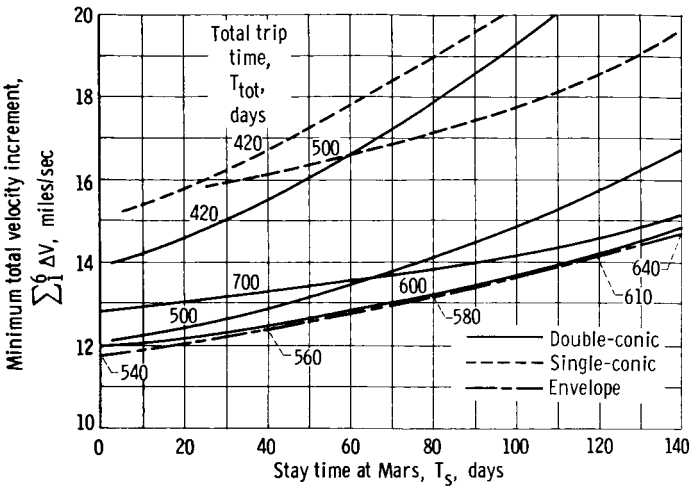

Figure 12. - Effect of stay time at Mars on minimum total velocity increment. Optimum single- and double-conic trips in 1980.

ries in 1980. A stay time of 40 days was chosen to be consistent with existing single-conic round-trip data (ref. 2). It will be noted that the single-conic trajectories (dashed lines) are represented by three distinct curves. The first curve (at shortest trip times) corresponds to fast trips in which the spacecraft describes a total central angle equal to the motion of the Earth ($N = 0$; cf. eq. (11)). The second curve, also with 40-day stays, involves longer trip times and the spacecraft travels exactly one revolution less than the Earth ($N = -1$). The transition region between these two curves involves central angles that are either very long or very short. The last curve represents near-Hohmann trips with $N = -1$ and stay times of 450 days. It is evident from the figure that double-conic trajectories (represented by the solid line) yield significantly lower $\sum \Delta V$ than the single-conic ones in the "fast" ($N = 0$) trip region. The saving becomes appreciable at about 380 days and increases to 6.5 miles per second out of 19 miles per second at 640 days. A new but very shallow minimum may be seen at 560 days, where $\sum \Delta V = 12.3$ miles per second, a saving of 3.8 miles per second over the single-conic trajectory minimum. At trip times approaching 700 days, single-conic trajectories represented by the second dashed curve ($N = -1$) become competitive with the double-conic trajectories. The double conics are not advantageous for trip times greater than about 700 days. The lowest $\sum \Delta V$ of all corresponds to Hohmann-type round trips with long trip times (850 to 1000 days) and long stay times at Mars (e.g., 450 days).

Effect of stay time at Mars. - In figure 12, the $\sum \Delta V$ is plotted against the stay time at Mars for 420-, 500-, 600-, and 700-day round trips. The solid curves represent double-conic trajectories while single-conics are denoted by the dashed curves. Here it is evident that the double-conic trajectories reduce $\sum \Delta V$ at a given trip time over a wide range of stay times. The reduction, however, is somewhat less pronounced at the longer stay times. It is of interest to note that if double-conic trajectories are used, a 500-day trip with a 130-day stay has the same $\sum \Delta V$ as a 500-day single-conic trip with a stay time of only 40 days.

The dot-dashed envelope curve on the lower part of the figure represents the lowest $\sum \Delta V$ obtainable with given stay times using double-conic trajectories in the "fast" ($N = 0$) trip region. An additional parameter, the trip time, was left open in obtaining this curve. The optimal values of T_{tot} corresponding to these trip times, as indicated by the markers along the envelope curve, range from 540 days ($T_s = 0$) to 640 days ($T_s = 140$). There is clearly very little incentive for considering trip times longer than about 550 days

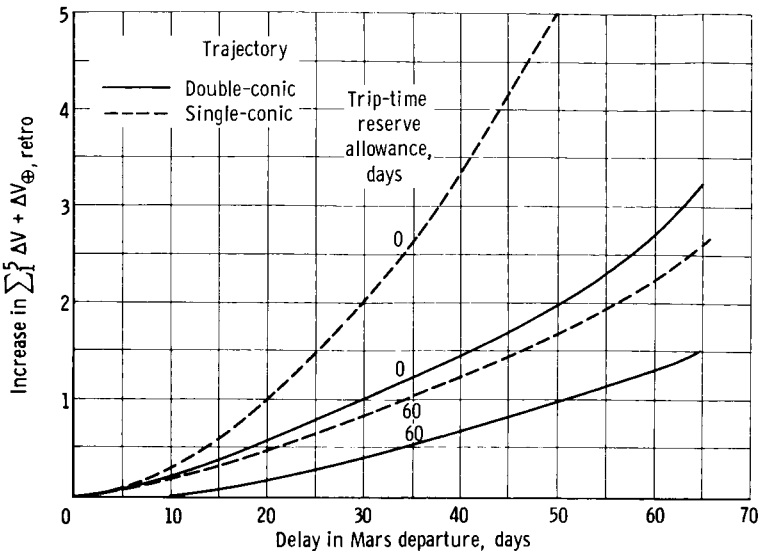

Figure 13. - Effect of delayed departure from Mars on minimum total velocity increment. Optimum single- and double-conic trips in 1980. Total trip time, 500 days; stay time, 40 days; Earth atmospheric entry velocity, $V_{\oplus e} \leq 45\,000$ feet per second.

unless very long stay times are required.

Delayed departure from Mars. - The trajectories discussed up to this point are characterized by the use of advance planning to select the most favorable transit time and central angle distribution for each chosen value of T_{tot} and T_s. A realistic flight plan, however, should be flexible enough to permit a safe return in spite of a minor mishap. Delayed departure from Mars will be discussed here as a typical example of the many types of safe-return problems that might be considered. This could become necessary for many plausible reasons, which include (1) rendezvous difficulty in returning a landing partly to the mother ship and (2) a minor propulsion system malfunction during nuclear engine startup. Either of these problems could require a considerable time delay for correction or repair.

The problem of delayed departure is similar to an extension of stay time except that only the inbound transfer can be reoptimized in response to the changed trajectory requirements. Figure 13 compares the $\sum \Delta V$ increase for single- and double-conic trajectories for delays in departure ranging up to 70 days. The comparison is based on planned minimum $\sum \Delta V$ single- and double-conic trips in 1980 with a 500-day duration and a 40-day stay time at Mars. Two cases were considered for each type of trajectory: First it was assumed that the round trip, including the delay, must be completed within the original 500-day period, and second that the round-trip time can be extended by as much as 60 days (to 560 days). With no time extension, both single- and double-conic trajectories require increased $\sum \Delta V$ for late departure, but the increase is considerably reduced if double-conic trajectories are used. If the trip time can be extended to 560 days, the increase is smaller for both types, but again the increase for the double-conic trajectory is considerably less than it is

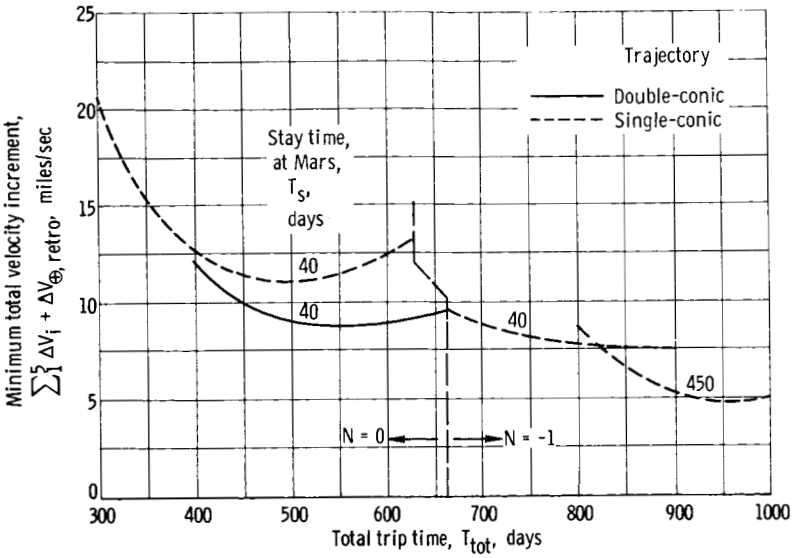

Figure 14. - Effect of atmospheric braking at Earth. Earth entry velocity, $V_{\oplus e} \leq 52\,000$ feet per second on round trips to Mars.

for single conics. This comparison shows that the $\sum \Delta V$ increase for departure delays can be cut by a factor of about 2 by using double-conic trajectories. This comparison is for trajectories which use propulsive braking at Earth, or atmospheric braking from velocities up to 45 000 feet per second. The difference is smaller for higher entry velocities.

Atmospheric braking. - It was shown above that double-conic trajectories can be used to produce large reductions in the all-propulsive $\sum \Delta V$ at trip and stay times of interest and to mitigate the effect of unexpected delay in Mars departure. It is well known that atmospheric braking can also be used to reduce $\sum \Delta V$. This section will consider the propulsive velocity increments and atmospheric entry velocities that occur when double-conic trajectories are used in combination with atmospheric braking at Earth return.

The combination of atmospheric braking with double-conic trajectories may be assessed according to two criteria, that is, the $\sum \Delta V$ savings compared to the all-propulsive double-conic case and compared to the single-conic trajectory with equal atmospheric braking. The results of these comparisons depend entirely on the allowable entry velocities. Assuming 37 000 feet per second as a limit (Apollo technology), single- and double-conic trajectories would benefit equally; the curves that were shown in figure 11 would simply be shifted downward by about 2 miles per second without affecting the relative advantage of double-conic trajectories. If the entry velocity is unrestricted, however, the double-conic trajectories are not appreciably better than single conics. In this case the search and optimization procedure described previously yields results approaching single-conic transfers. The associated entry velocities, however, are extremely high (e.g., about 70 000 fps for the 500-day trip). Assuming an intermediate limit, $V_{e\oplus} \leq 52\,000$ feet per second, leads to the results shown in figure 14. Here $\sum \Delta V$ is plotted against T_{tot} as it was in figure 10; com-

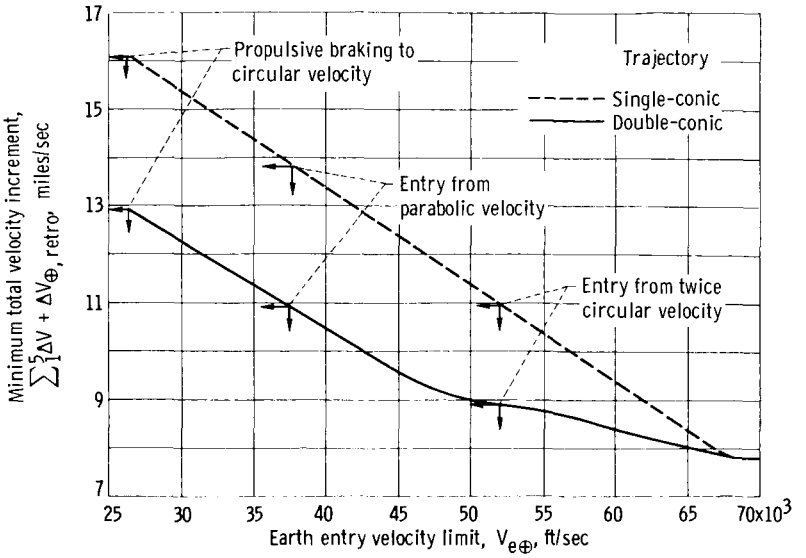

Figure 15. - Effect of allowable Earth atmospheric entry velocity on minimum total velocity increment for 500-day round trips to Mars in 1980. Stay time, 40 days.

parison of these two figures indicates that the $\sum \Delta V$ reduction due to double-conic trajectories is available over the same wide range of trip times as in the all-propulsive case. The minimum $\sum \Delta V$ for the double-conic is 2.5 miles per second below the minimum available from a single-conic trajectory with the same entry velocity limit. This is also a saving of 3.5 miles per second as compared to the all-propulsive double-conic case.

The variation of $\sum \Delta V$ with allowable Earth atmospheric entry velocity is further illustrated in figure 15, where the 500-day trip with a 40-day stay is used as an example. The $\sum \Delta V$ is plotted against $V_{e\oplus}$ using dashed and solid curves to represent single- and double-conic trajectories, respectively. The maximum advantage (3.2 miles/sec) that occurs in the all-propulsive braking case is maintained up to an entry velocity of about 45 000 feet per second, and thereafter decreases as $V_{e\oplus}$ is further increased. A retromaneuver is needed to reach entry velocities below 45 000 feet per second. The orbit elements of the Mars-Earth transfer are approximately constant for entry velocities from 25 000 to 45 000 feet per second; the reduction in $\sum \Delta V$ as $V_{e\oplus}$ increases in this range is simply due to the proportional decrease in the retromaneuver ΔV. If $V_{e\oplus} > 45\,000$ feet per second, no retromaneuver is used; instead, the transfer orbit elements are reoptimized to take full advantage of the higher $V_{e\oplus}$ limit.

From this example it may be observed that double-conic trajectories can be used in combination with atmospheric braking to produce attractive reductions in $\sum \Delta V$ without requiring excessive entry velocities. The advantage of double-conic over single-conic trajectories tends to decrease as the allowable Earth atmospheric entry velocity is increased.

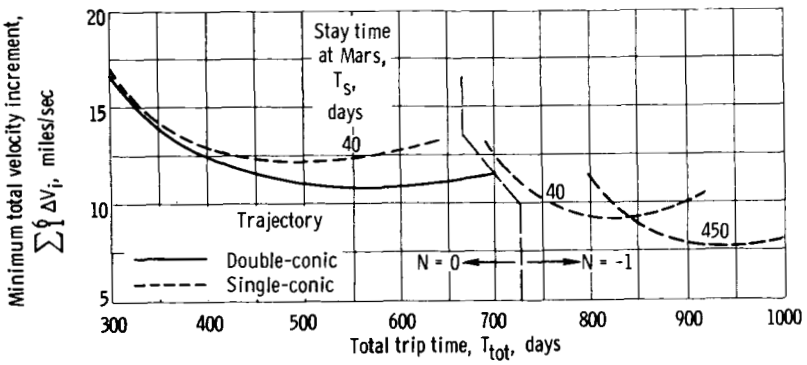

Figure 16. - Comparison of single- and double-conic round trips to Mars. All propulsive braking (1971).

Effect of synodic period. - Because of the eccentricity of Mars's orbit, its radius at opposition varies from 1.38 astronomical units in 1971 to 1.66 astronomical units in 1980. Optimal trips in the latter period involve greater radial and angular travel and thus tend to require a higher $\sum \Delta V$ than trips in other oppositions. Conversely, trips in 1971 are the least difficult. Trips in the difficult 1980 period were shown in the preceding figures. Figure 16 illustrates the variation of $\sum \Delta V$ with T_{tot} for all-propulsive trips in 1971 using solid lines for double-conic trajectories and dashed lines for single conics. Again, the double-conic trajectories yield appreciable reductions of $\sum \Delta V$ for trip times of 360 to 720 days. The reductions, however, are less pronounced than those found in 1980. The minimum $\sum \Delta V$ is decreased by 1.6 miles per second in this period (compared to 3.8 miles/sec in 1980). As was the case in 1980, there is little $\sum \Delta V$ advantage for double-conic trajectories if unrestricted Earth aerobraking capability is available.

It is pointed out in appendix B that the advantage of a double-conic over a single-conic trajectory increases as the angular and radial travel increase. Thus, the same factors that make 1971 an "easy" year also account for the less advantageous showing of double-conic trajectories.

Five-hundred-day single- and double-conic round trips are compared in figure 17 over a range of synodic periods. The ΔV sum for the minimum $\sum \Delta V$ all-propulsive trips within each synodic period is plotted against opposition year from 1971 to 1986. The double-conic trajectories produce a $\sum \Delta V$ reduction in all synodic periods, ranging from 1.2 miles per second in 1971 and 1986, to 3.2 miles per second in 1980. The net result is a pronounced flattening of the $\sum \Delta V$ requirement as a function of synodic period in addition to the general reduction in level.

Effect of trajectory profile. - It was illustrated in table III that the optimum travel angle and travel time distribution for fast ($N \approx 0$) Mars round trips are not necessarily symmetrical, and also that the assymetry is increased when the trajectory is reoptimized for double-conic transfers. The trips that were discussed for 1980 consisted of short-angle outward transfers and long-angle returns. These are termed "short-long" trips. Another class of round trips, "long-short," also exists, in which the angular relation is reversed.

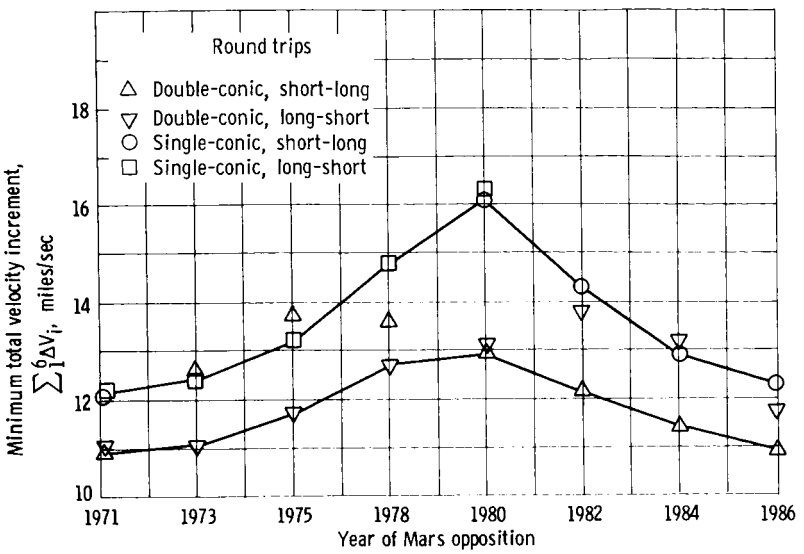

Figure 17. - Comparison of optimum single- and double-conic round trips to Mars in different synodic periods. Total trip time, 500 days; stay time, 40 days.

It is evident from figure 17 that the choice of trajectory profile has a significant effect on $\sum \Delta V$ in most synodic periods. For both single- and double-conic trajectories, the long-short profile yields minimum all-propulsive $\sum \Delta V$ from 1971 to 1980, while the short-long profile is advantageous between 1980 and 1986. (As shown in appendix B, the more difficult profile in a given period is the one which requires the greater radial and angular travel.)

For the trip time chosen in this example, the double-conic trajectories possess distinct local-minimum long-short and short-long profiles in every synodic period. (In 1980, for instance, the local minimum for the short-long profile is illustrated by the lower circle symbol on fig. 10.) In most years only one trajectory profile yields a local minimum $\sum \Delta V$ for single-conic trips.

These facts have several implications. In a given synodic period, double-conic trajectories not only reduce the $\sum \Delta V$, but also reduce the variations between the individual ΔV's. The $\sum \Delta V$ penalty in designing for the worst synodic period compared to the best, is only 2 miles per second, if double-conics are used. Moreover, the individual ΔV distribution, being relatively uniform, would not be significantly affected when the transition from the long-short to the short-long profile is made.

By contrast, with single-conics, the $\sum \Delta V$ penalty for designing for the worst period is over 4 miles per second. In addition, the individual ΔV distribution, being highly nonuniform (cf. table III), would be drastically modified in making the transition from the long-short to the short-long trajectory profile.

These considerations suggest that by using double-conic trajectories, a

standardized spacecraft could be designed which could accomplish a mission in any synodic period, or a sequence of missions covering many synodic periods.

Comparison with Venus swingby trajectories. - Another efficient new class of Mars round-trip trajectories is the Venus swingby described in references 9 and 10. These trajectories incorporate a close passage by Venus during the long-angle leg of a round trip. They resemble the present trajectories in that low $\sum \Delta V$ long-angle transfers consist of two conic arcs; the gravitational force acting during the Venus passage replaces the midcourse propulsion as the

TABLE IV. - COMPARISON OF DOUBLE-CONIC AND VENUS SWINGBY TRAJECTORIES FOR ROUND TRIPS TO MARS

[Propulsive braking; low circular parking orbits; stay time, 10 days; optimum total trip time.]

Launch year	Type of trajectory	Minimum total velocity increment, $\sum_1^6 \Delta V$, miles/sec	Optimum total trip time, T_{tot}, days	Velocity increments					
				Outbound transfer			Return transfer		
				ΔV_1 (date, 244-)	ΔV_2 (date, 244-)	ΔV_3 (date, 244-)	ΔV_4 (date, 244-)	ΔV_5 (date, 244-)	ΔV_6 (date, 244-)
[a]1975	Single-conic	16.37	430	2.58 (2670)	------	2.68 (2840)	3.14 (2850)	------	7.97 (3100)
[b]1975	Double-conic	10.81	510	2.50 (2366)	1.60	2.71 (2642)	1.87 (2652)	------	2.13 (2867)
[a]1975	Venus swingby	11.18	518	2.61 (2670)	------	3.35 (2820)	2.24 (2830)	Pass Venus (3050)	2.98 (3188)
[a]1978	Single-conic	16.80	430	2.51 (3440)	------	2.91 (3620)	3.15 (3630)	------	8.23 (3870)
[b]1978	Double-conic	11.49	517	2.53 (3109)	2.06	2.77 (3397)	1.86 (3407)	------	2.27 (3625)
[a]1978	Venus swingby	13.05	699	3.23 (3081)	Pass Venus (3319)	3.23 (3458)	1.87 (3468)	------	4.72 (3780)
[a]1980	Single-conic	15.77	430	2.42 (4190)	------	3.18 (4380)	2.96 (4390)	------	7.21 (4620)
[b]1980	Double-conic	11.88	550	2.22 (4180)	------	1.63 (4440)	3.06 (4450)	2.29	2.68 (4730)
[a]1980	Venus swingby	10.40	540	2.85 (3840)	Pass Venus (3996)	3.45 (4120)	1.45 (4120)	------	2.65 (4380)

[a]Ref. 10; minimum weight.

[b]Present analysis; minimum $\sum_1^6 \Delta V$.

means of switching from one arc to the next.

The Venus swingby trajectories presented in reference 10 are not directly comparable to the present results because they were obtained on the bais of minimum gross weight for a particular space vehicle configuration and for a mission profile (atmospheric braking at Mars) that was not studied herein. A limited comparison (table IV) nevertheless yields some interesting similarities and contrasts:

(1) In comparison with single-conic trajectories, both double-conic and Venus swingby trajectories offer significant $\sum \Delta V$ savings together with moderate Earth-approach velocities. Only one of the double-conic or swingby trajectories shown in table IV (the 1978 swingby) would benefit from an Earth aerobraking capability greater than about 42 000 feet per second. The single conics would need 65 000 to 75 000 feet per second of aerobraking capability to be competitive.

(2) In 1975, the optimum double-conic and Venus swingby trajectories will require comparable values of $\sum_1^6 \Delta V$ and trip time.

(3) In 1978, the double-conic trajectory appears to have a clear advantage from the standpoints of both $\sum_1^6 \Delta V$ and trip time.

(4) In 1980, by contrast, the Venus swingby offers a decidedly lower value of $\sum_1^6 \Delta V$ for comparable trip times.

(5) It may be noted that there is a considerable difference in the Mars-arrival dates (and hence, the Martian season) for double-conic and swingby trajectories. This may be significant from the standpoint of mission objectives.

Although 1980 is the most difficult period for double-conic trajectories, it is especially favorable for swingbys. In such years, Venus is in the most appropriate position relative to Earth and Mars. It is then possible to obtain many of the characteristics of double-conic trajectories without midcourse propulsion. In other years, however, the elimination of midcourse propulsion is offset by less favorable configurations of Venus.

On the other hand, double-conic trajectories owe their efficiency to a careful optimization of the location, magnitude, and direction of the midcourse ΔV. This process does not depend on the configuration of a third planet and therefore yields consistent results in all synodic periods.

These examples indicate that double-conic and Venus swingby trajectories are comparable techniques whose relative merits depend strongly on the synodic period and possibly on mission objectives. Further comparisons between them will depend on accounting for both mission factors and trajectory characteristics in a consistent manner. Finally, the possibility cannot be excluded that hybrid trajectories, which would incorporate both Venus swingby and double-conic portions, may yield a lower $\sum \Delta V$ than either double conics or Venus swingbys alone.

CONCLUSIONS

An efficient class of high-thrust interplanetary trajectories has been analyzed in which a midcourse impulse is used to reduce the total velocity requirement. Each one-way plane-to-planet transfer consists of two heliocentric conic sections and requires three impulses rather than the customary two.

For one-way trips to Mars, these double-conic trajectories yield lower total velocity increments than conventional single-conic trajectories if the heliocentric travel angle is greater than about 4 radians. The improvement is most noticeable at long transit times and is large enough to produce new relative minima in the long-angle region for transit times greater than 350 days. None of the new time-constrained minima, however, are lower than that resulting from the classical single-conic Hohmann transfer.

Although Hohmann-type round trips of about 3-year duration represent an absolute minimum $\sum \Delta V$, the double-conic trajectories can be used to produce notable reductions in $\sum \Delta V$ for round trips of 1 to 2 years. The reductions are largest for all propulsive trips but are still significant when atmospheric braking is used at Earth return. The greatest savings occur in the most difficult synodic periods; consequently, the variation of $\sum \Delta V$ with synodic period is decreased by a factor of about 2. The variation of the individual velocity increments between long-short and short-long trips is also reduced by a large amount. These properties of double-conic trajectories may imply gross-weight reductions for an interesting class of trips and enhance the possibility of using a standard spacecraft for missions in many synodic periods.

A comprehensive mission study is required to more precisely evaluate the advantages and applicability of double-conic trajectories as compared with Venus swingby and conventional single-conic trajectories for specific Mars missions. Additional effort is indicated to investigate the utility of double-conic trajectories for missions to Venus and the major planets, and to determine whether two or more midcourse impulses could be used to obtain still greater reductions in $\sum \Delta V$.

Lewis Research Center,
National Aeronautics and Space Administration,
Cleveland, Ohio, September 28, 1965.

APPENDIX A

COMPUTATION OF PLANET POSITION AND VELOCITY

Elliptic Planet Orbits

The elements of a transfer trajectory, and the associated velocity increments, may be computed in terms of the travel time if the position and velocity vectors at each planet terminal are known. These quantities may in turn be derived from the date of encounter at each planet terminal by using the planet-orbit data shown in table V (obtained from ref. 3).

Only one more parameter, the true anomaly $\theta(D)$, is required to compute the planet position and velocity at the encounter date. The elapsed time since the last perihelion passage ΔT_p is

$$\Delta T_p = D - D_{pr} + N\tau \tag{A1}$$

where $N(= 0, \pm 1, \pm 2, \ldots)$ is chosen to obtain the smallest positive value of ΔT_p. An assumed or estimated value of $\theta(D)$, inserted in the time equation (5), yields a trial value that may be compared to equation (A1). The error is then used to obtain a better estimate of $\theta(D)$; this iteration cycle is continued until the error is within acceptable tolerances. After the n^{th} step,

$$\theta(D)\Big|_{n+1} = \theta(D)\Big|_{n} + C_n \, \delta T_n \tag{A2}$$

where the error is given by

$$\delta T_n = \Delta T_p - \Delta T_p\Big|_n \tag{A3}$$

and the coefficient by

TABLE V. - ORBIT ELEMENT AND PHYSICAL DATA FOR EARTH AND MARS

Planet	Perihelion radius, ρ_p, astronomical units	Eccentricity, e	Perihelion date (ref), D_{pr}, Julian day	Orbital period, τ, days	Circular velocity at 1.1 planet radii, V_{po}, miles/sec	[a]Relative displacement of perihelion, α_p, rad
Earth	0.9833	0.0167	2444242	365.2	4.670	0
Mars	1.3814	.0934	2443951	687.5	2.121	4.70

[a]Measured counterclockwise from Earth perihelion.

$$C_n = \frac{\theta(D)\Big|_n - \theta(D)\Big|_{n-1}}{\delta T_n} \approx \frac{\partial\theta(D)}{\partial T} \qquad n \geq 1 \qquad \text{(A4)}$$

Since the planet orbits are nearly circular, the planet mean motions ($\langle M\rangle \triangleq 2\pi/\tau$) may be used to obtain good starting values which lead to very rapid convergence:

$$\left.\begin{aligned} \theta(D)\Big|_0 &= \langle M\rangle\, \Delta T_p \\ C_0 &= \langle M\rangle \end{aligned}\right\} \qquad \text{(A5)}$$

With the true anomaly determined in this manner, the planet radius, velocity, and path angle at the encounter date may be computed directly from equations (6) and (7). Finally, the polar travel angle β may be calculated from the true anomalies of Earth and Mars. For an outward (Earth-Mars) transfer, β_{out} is the angle from Earth at the departure date measured counterclockwise to Mars at the arrival date; that is,

$$\beta_{out} = \alpha_p + \theta_{\sigma'}(D_{\sigma'}) - \theta_{\oplus}(D_{\oplus}) + 2\pi N \qquad \text{(A6)}$$

where α_p is the angle from Earth's perihelion to Mars' perihelion. For an inward transfer, the angle is measured from Mars to Earth, thus

$$\beta_{inw} = 2\pi N - \left[\alpha_p + \theta_{\sigma'}(D_{\sigma'}) - \theta_{\oplus}(D_{\oplus})\right] \qquad \text{(A7)}$$

In either case, N(= 0, ±1, ±2, . . .) is chosen to obtain the smallest positive value of β.

Circular Planet Orbits

If the planet orbits were circular, the perihelion dates and positions and the true anomalies used above are not well defined. In that case, it is convenient to define $\alpha_p = 0$ and measure the planet central angles and encounter date relative to opposition. The iteration cycle just described then yields an exact result in one step; equations (A6) and (A7) reduce to

$$\beta_{out} = M_{\oplus}\, \Delta T_{\oplus-\sigma'} - (D_{\sigma'} - D_{opp})(M_{\oplus} - M_{\sigma'}) + 2\pi N \qquad \text{(A8)}$$

for an outward transfer, and

$$\beta_{inw} = M_{\oplus}\, \Delta T_{\oplus-\sigma'} + (D_{\sigma'} - D_{opp})(M_{\oplus} - M_{\sigma'}) + 2\pi N \qquad \text{(A9)}$$

for inward transfer, upon noting that D_{pr} in equation (A1) is replaced by D_{opp}.

These results may be used as "inputs" for the transfer trajectory calculation shown in the Analysis section.

APPENDIX B

SIMILARITY OF EARTH-MARS TRAJECTORIES IN DIFFERENT SYNODIC PERIODS

Similarity Conditions for Earth-Mars Transfers

For circular-coplanar planet orbits, each outward transfer possesses an inward counterpart having equal terminal radii, travel angle, and travel time when the Mars encounter dates are related by

$$D_{\sigma',inw} = 2D_{opp} - D_{\sigma',out} \tag{B1}$$

as may be seen by equating (A8) and (A9) with

$$\beta_{out} = \beta_{inw}$$

and

$$\Delta T_{\oplus-\sigma'} = \Delta T_{\sigma'-\oplus}$$

The counterpart trajectories thus obtained are geometrical mirror images of one another and are dynamically similar.

This mirror-image property between inward and outward transfers with equal travel times does not hold, in general, for the elliptic-coplanar orbits considered herein. The property does hold, however, in one special case, when the lines of apsides of the two planet orbits coincide with the line of opposition. In this case, because of symmetry, the average planet motions are the same on either side of opposition, so that equations (A8) and (A9) when combined as above will still yield equation (B1). In this case, the counterpart trajectories are still geometrical mirror images obtained by reflection about the common line of opposition and apsides. They have equal terminal radii, travel angle and travel time, and are dynamically similar in that the ΔV at a given terminal planet is the same.

This condition is well approximated in 1980 since Mars is close to its aphelion at the opposition date (2444295) and the Earth's orbital eccentricity is very small compared to Mars'. This observation justifies the dual interpretation of the trajectory data in tables I and II as stated in the RESULTS AND DISCUSSION. It should be noted in addition that the dual or mirror-image property holds in all synodic periods, not just in 1980, as long as the reference date 2444295 is used. That is, an outward transfer which reaches Mars 100 days before the 1978 opposition would have a mirror image counterpart in an inward transfer departing Mars 100 days after the 1982 opposition; the two transfers would have equal travel times and nearly the same travel angle and terminal radii.

Effect of Synodic Period on Earth-Mars Trips

Mars' heliocentric radius at opposition increases from 1.38 astronomical units in 1971 to 1.68 astronomical units in 1980, and then decreases again from 1980 to 1989. For a given travel time and angle, the transfer requiring the greater radial travel will require the higher $\sum \Delta V$ simply because a greater distance must be covered in an equal time interval.

Round trips with $N = 0$ may be conveniently classified according to the distribution of the total available travel angle (eq. (3)) between the outward and return legs. If the outward travel angle β_{out} is larger than β_{inw}, the trip is referred to as a long-short round trip. Similarly, short-long trips have a long-angle return leg.

Figure 17 shows that the choice of trajectory profile, that is, short-long or long-short, has a sizable effect on round trip $\sum \Delta V$ in most synodic periods. For either single- or double-conic trajectories, the long-short profile is advantageous between 1971 and 1980, while the short-long profile yields lower $\sum_1^6 \Delta V$ from 1980 through 1986. This effect may be understood by considering the following arguments.

(1) As previously mentioned, the radius of Mars at opposition increases from 1.38 astronomical units in 1971 to 1.66 astronomical units in 1980, and then decreases again from 1980 to 1986.

(2) For fast round trips, the angular matching requirements discussed in the Analysis section require the spacecraft to be at Mars within a period of roughly ±150 days from opposition.

(3) In a given synodic period, the long-short profile occupies the first part of this ±150-day band, corresponding to early arrival at Mars. Conversely, the short-long profile represents late arrival in the latter part of the band.

(4) A short-long trip is therefore likely to reach the vicinity of Mars as much as 300 days later than a comparable long-short trip.

(5) The radius of Mars' orbit varies an appreciable amount during this period except in oppositions such as 1971 or 1980 when Mars is near one of its apses.

(6) Thus, during the cycle of opposition (1971 - 1980) when the radius of Mars' orbit is increasing, a short-long trip, by arriving later, is required to travel a greater radial distance than the long-short profile. Since the angular velocity of Mars is decreasing during this period, the short-long trajectory must also describe longer central angles to match the Earth's motion. The short-long trip is therefore more difficult than the long-short between 1971 and 1980. The reverse is true during the decreasing cycle between 1980 and 1989. For an opposition such as 1980 when Mars is near an apse, the flight profiles are dynamically similar and therefore require about the same $\sum \Delta V$.

REFERENCES

1. Knip, Gerald, Jr.; and Zola, Charles L.: Three-Dimensional Sphere-of-Influence Analysis of Interplanetary Trajectories to Mars. NASA TN D-1199, 1962.

2. Knip, Gerald, Jr.; and Zola, Charles L.: Three-Dimensional Trajectory Analysis for Round-Trip Missions to Mars. NASA TN D-1316, 1962.

3. Anon.: Space Flight Handbooks. Vol. III: Planetary Flight Handbook. NASA SP-35, 1963.

4. Lawden, D. F.: Optimal Trajectories for Space Navigation. Butterworth Sci. Pub., 1962.

5. Fimple, W. R.: Optimum Midcourse Plane Changes for Ballistic Interplanetary Trajectories. AIAA J., vol. 1, no. 2, Feb. 1963, pp. 430-434.

6. Willis, Edward A., Jr.: New Class of Optimal Interplanetary Trajectories with Specified Trip Time. Paper No. 65-66, AIAA, Jan. 1965.

7. Ehricke, K. A.: Principles of Guided Missle Design. Vol. 1 of Space Flight, G. Merrill, ed., D. Van Nostrand Co., Inc., 1960, pp. 332-344.

8. Wilde, D. J.: Optimum-Seeking Methods. John Wiley and Sons, Inc., 1964, pp. 128-145.

9. Sohn, Robert L.: Venus Swingby Mode for Manned Mars Missions. J. Spacecraft and Rockets, vol. 1, no. 5, Sept.-Oct. 1965, pp. 565-567.

10. Deerwester, Jerry M.: Initial Mass Savings Associated with the Venus Swingby Mode of Mars Round Trips. Paper No. 65-89, AIAA, 1965.